Structural evolution of the Cruzeiro do Nordeste shear zone (NE Brazil): Brasiliano-Pan-African- ductile-to-brittle transition and Cretaceous brittle reactivation

Tiago Siqueira de MIRANDA[a]* (tiago.smiranda@ufpe.br)
Sérgio Pacheco NEVES[a] (serpane@hotlink.com.br)
Maria Alcione Lima CELESTINO[b] (alcionelimma22@gmail.com)
Nick M. W. ROBERTS[c] (nirob@bgs.ac.uk)
[a]Department of Geology, Federal University of Pernambuco, Recife, PE, 50740-530, Brazil
[b]Geosciences Graduate Program, Federal University of Pernambuco, Recife, PE, 50740-530, Brazil
[c]Geochronology and Tracers Facility, British Geological Survey, Environmental Science Centre, Nottingham, NG12 5GG, UK
*Corresponding author; e-mail: tiago.smiranda@ufpe.br; telephone: +55 81 98743-9197; postal address: Av. da Arquitetura, 953-995 - Cidade Universitária, Recife - PE, 50740-540, Brazil.

Abstract

The Borborema Province (NE Brazil) is characterized by the development of continental-scale transcurrent shear zones related to the Neoproterozoic Brasiliano-Pan-African Orogeny. These shear zones commonly border Cretaceous intraplate sedimentary basins . This work presents a structural and microstructural study of the Cruzeiro do Nordeste shear zone (CNSZ), which limits the northern border of the Jatobá Basin. The ductile deformation of the CNSZ is marked by high-angle, ENE-trending foliation bearing subhorizontal stretching lineation, with numerous kinematic indicators showing dextral shearing. We documented a continuous transition from high-temperature (high-T) to low-temperature (low-T) (c. 650 °C to c. 300 °C) ductile fabrics characterized, at the high-T end, by quartz recrystallization by grain boundary migration and feldspar recrystallization by subgrain rotation, and, at the low-T end, by bulging recrystallization of quartz and extensive fracturing of feldspars. The cooler semi-brittle to brittle deformation superimposed on the mylonites is characterized by conjugate pairs of strike-slip mesoscopic faults. The orientation of these faults (WNW-ESE, dextral, and N-S, sinistral) suggests they were formed under the same stress field than the ductile fabrics and thus evidence a continuum deformational from the ductile to the brittle field associated with exhumation during transcurrent tectonics. Brittle reactivation of the CNSZ is characterized by normal faults overprinting the mylonitic foliation. We report a U-Pb age from fault-hosted calcite slickenfibres of 135 ± 4.7 Ma, which provides constraints on the timing of brittle reactivation that can be associated with opening of the South Atlantic Ocean.

Keywords: Borborema Province; mylonite; Jatobá Basin; cataclasite ; U-Pb; c alcite

1. Introduction

Most Phanerozoic orogenic belts are characterized by late to post-orogenic gravitational collapse (Dewey, 1988; Leech, 2001; Rey et al., 2001; Jadamec et al., 2007; Vanderhaeghe, 2012). However, though common, widespread post-orogenic extension is not recorded in several orogenic belts worldwide. For instance, in many Brasiliano-Pan-African belts, the last stages of orogenic evolution are not manifested by the development of large extensional detachment zones. Instead, crustal-scale strike-slip shear zones are the main expression of the late-orogenic tectonic deformation, locally associated with the formation of transtensional basins and intrusion of granites with A-type affinity by the end of the orogenic activity. This is the case, for instance, of the

Kaoko Belt in Namibia (e.g., Goscombe et al., 2003; Konopásek et al., 2005), the Central African Orogenic Belt in Cameroon (e.g, Ngako et al., 2003), the Tuareg Shield in Hoggar, Algeria (e.g., Paquette et al., 1998), and the Borborema Province in northeastern Brazil (e.g., Araújo et al., 2001; Hollanda et al., 2010; Castro et al., 2012). These observations suggest that the increase of the vertical stress due to the thickening of the orogenic lithosphere was not effective enough to overcome the horizontal stresses and thus to trigger gravitational collapse. Continued transcurrent deformation during cooling of the belts implies that the intermediate main stress axis remained vertical during exhumation, which is possible if the horizontal tectonic stress did not decrease fast enough. In consequence, a given horizontal surface can be brought to progressively shallower crustal levels and thus record ductile to brittle deformation (e.g., West et al., 1997; Stewart et al., 2000; Clerc et al., 2017).

The Borborema Province is an ideal place to study the ductile-brittle transition since it contains numerous well-exposed NE- to E-trending crustal-scale transcurrent shear zones (Vauchez et al., 1995). These shear zones have been the subject of several previous studies that highlighted their medium- to high-temperature fabrics (e.g., Neves, 1991; Vauchez and Egydio-Silva, 1992; Corsini et al., 1996; Neves and Mariano, 1999; Silva and Mariano, 2000; Archanjo et al., 2002, 2008; Viegas et al., 2014; Neves et al., 2018). However, there is a general lack of information concerning their cooler semi-brittle to brittle deformation. In fact, brittle structures are usually ascribed to reactivation during the Cretaceous (e.g., Castro et al., 2008; Nogueira et al., 2015) or even to neotectonic events (e.g., Ferreira et al., 2008; Bezerra et al., 2014). The aim of this paper is to fill this gap by describing a case study of ductile-brittle transition and brittle deformation of the Cruzeiro do Nordeste shear zone (CNSZ) that limits the northern border of the Jatobá Basin, NE Brazil (Fig. 1). We demonstrate that ductile and brittle-ductile structures were formed under the same stress field, showing that deformation related to the Brasiliano Orogeny persisted into the Paleozoic.

The interior basins of northeastern Brazil such as Araripe, Rio do Peixe, Jatobá and Fátima are surrounded by Precambrian shear zones (e.g., Pernambuco, Patos, Afogados da Ingazeira and Cruzeiro do Nordeste shear zones) (Fig. 1). Furthermore, brittle reactivation of these shear zones played an important role in the tectonic evolution of the sedimentary basins. Here, we propose that the Jatobá rift system was tectonically configured by the brittle-ductile deformation associated with the Brasiliano orogenic cycle. As such, we discuss how to distinguish brittle structures formed at the late stages of this orogeny, and those resulting from rifting during the Cretaceous. In addition, we report a U-Pb age from strike-slip fault-hosted calcite, which provides constraints on the age of Cretaceous brittle reactivation of the CNSZ.

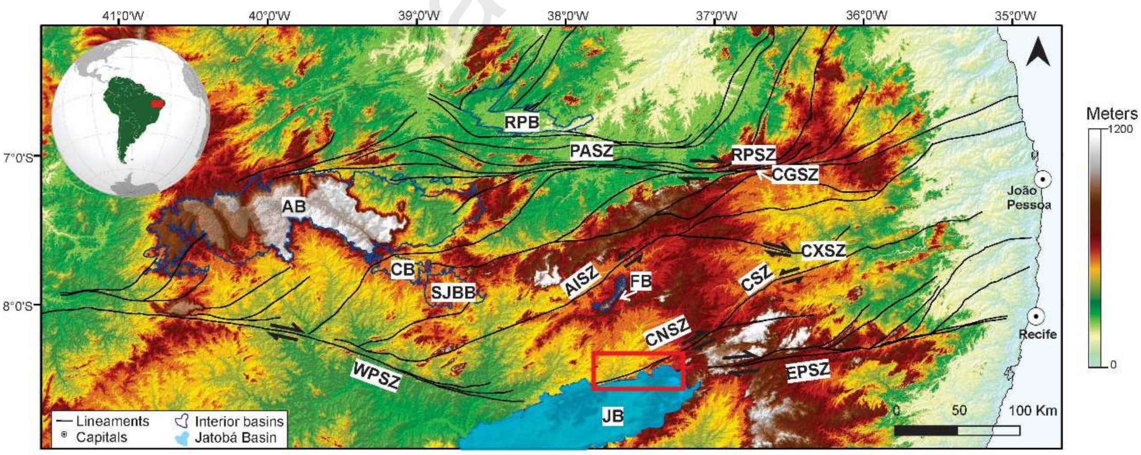

Figure 1. Digital elevation model of the Central Borborema Subprovince showing the principal intraplate basins of northeastern Brazil. PASZ, Patos shear zone; EPSZ, East Pernambuco shear zone; WPSZ, West Pernambuco shear zone; CNSZ, Cruzeiro do Nordeste shear zone; CSZ, Congo shear zone; AISZ, Afogados da Ingazeira shear zone; RPSZ, Remígio-Pocinhos shear zone; CGSZ, Campina Grande shear zone; CXSZ, Coxixola shear zone; JB, Jatobá Basin; FB, Fátima Basin; SJBB, São José do Belmonte

Basin; CB, Cedro Basin; AB, Araripe Basin; RPB, Rio do Peixe Basin. Red rectangle marks the study area.

2. Geological setting

2.1. Geometry, kinematics and geochronology of shear zones

The Borborema Province was the locus of intense tectonic activity during the Late Neoproterozoic to early Paleozoic Brasiliano Orogeny (e.g., Brito Neves et al., 2000; Van Schmus et al., 2008, Neves, 2015 and references therein). The most conspicuous feature of this orogeny was the development of tens to hundreds of kilometers-long strike-slip shear zones that are clearly visible in aerogeophysical, satellite and radar imagery and aerial photographs (Fig. 2); these constitute the so-called Borborema shear zone system (Vauchez et al., 1995).

The large Patos and Pernambuco shear zone systems (PASZ and PSZ, respectively) are now routinely used to subdivide the Borborema Province into the Northern, Central and Southern subprovinces (e.g., Santos et al., 2010; Van Schmus et al., 2011; Neves, 2015). Although most simplified regional maps published in recent papers continue to show these shear zones as single, continuous structural features, several studies reveal a more complex picture (Neves and Mariano, 1999; França et al., 2019). The E-trending Patos shear zone proper consists of a mylonitic belt up to 25 km in width whose foliation curves and grades eastwards into the fabric of the transpressional NE-trending Seridó Belt (Corsini et al., 1991; Archanjo et al., 2002, 2013). In contrast, its eastern branch, the Remígio-Pocinhos shear zone, is a narrow shear zone that changes strike eastwards and acquires NE orientation (Souza et al., 2006). Similarly, the Pernambuco system is composed of two distinct segments: the up to ten-km wide ESE-trending West Pernambuco shear zone (Vauchez and Egydio-Silva, 1992) and the narrower East Pernambuco shear zone that fades away westwards before reaching the Jatobá Basin (Neves and Mariano, 1999).

In the Central Subprovince and northern portion of the Southern Subprovince, E- to ENE-trending shear zones and NE- to NNE-trending shear zones form a conjugate set with dextral and sinistral kinematics, respectively (Fig. 1). The timing of strike-slip activity, mainly determined thorough zircon dating of synkinematic plutons or of syn-shear leucosomes, is available for only a few examples. In the East Pernambuco shear zone and associated subsidiary sinistral shear zones, Pb-Pb and conventional U-Pb zircon ages of early syn-tectonic plutons range from 592 to 587 Ma (Guimarães et al., 2004; Neves et al., 2004), and syntectonic plutons displaying evidence of wrench deformation at lower temperature conditions provided U-Pb ages in the interval 573-562 Ma (Neves et al., 2008; Neves et al., 2020). In the Campina Grande shear zone, a syntectonic pluton yielded a U-Pb zircon age of 576 ± 3 Ma (Archanjo et al., 2008). In the Patos shear zone, recrystallized zircon rims recovered from leucosomes of melt-bearing mylonites, combined with the crystallization age of synkinematic plutons, indicate an interval of 566-558 Ma for the high-grade dynamic metamorphism (Viegas et al., 2013, 2014). $^{40}Ar/^{39}Ar$ biotite ages of 545-533 Ma provide the timing of metamorphic cooling following ductile deformation in the EPSZ (Neves et al., 2000) and are similar to $^{40}Ar/^{39}Ar$ muscovite ages (ca. 547 Ma) in the eastern portion of the Coxixola shear zone (Hollanda et al., 2010). In the western portion of this latter shear-zone, low-temperature ultramylonites provided $^{40}Ar/^{39}Ar$ muscovite ages of ca. 510 Ma (Hollanda et al., 2010), suggesting that shearing may have continued well into the Cambrian.

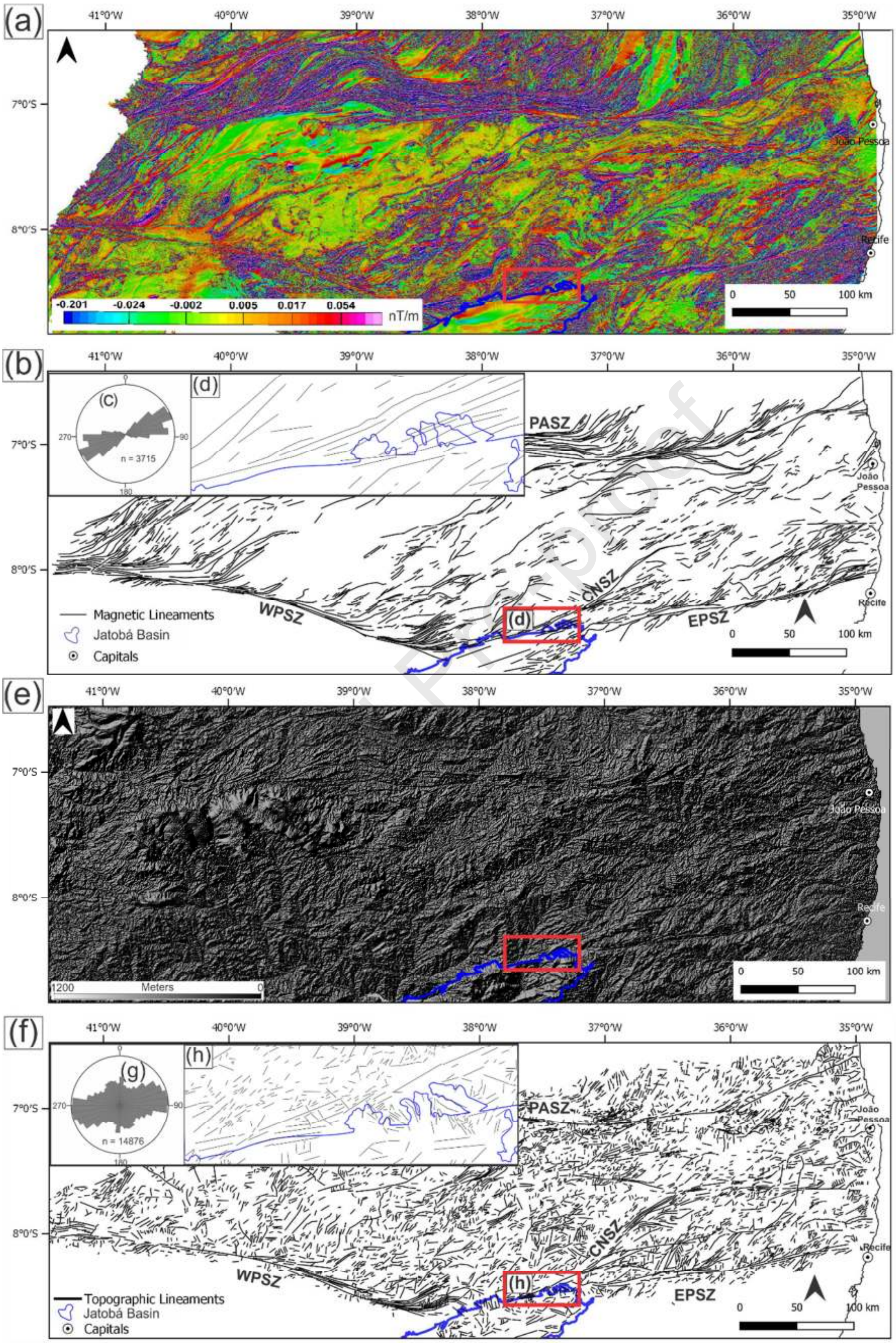

Figure 2. Aeromagnetic map (first derivative) (a) and the main magnetic lineaments (b) of the Central Subprovince of the Borborema Province. (c) Rose diagram of the

magnetic lineaments illustrating a preferential ENE-WSW direction. (d) Detail showing the study area. Digital elevation model of the Central Subprovince (e) showing the main topographic lineaments (f). (g) Rose diagram of the topographic lineaments illustrating a preferential ENE-WSW direction. (h) Detail showing the study area. PASZ, Patos shear zone; EPSZ, East Pernambuco shear zone; WPSZ, West Pernambuco shear zone; CNSZ, Cruzeiro do Nordeste shear zone. Sources: Brazilian Geological Survey (CPRM) and United States Geological Survey (USGS).

3. Cruzeiro do Nordeste shear zone

3.1.General characteristics

Previous work has considered the Congo-Cruzeiro do Nordeste shear zone system as a single, sinistral shear zone, inflecting southwestward from a NE trend to an ENE one (Santos et al., 2002; Santos and Acioly, 2010; Santos, 2012). However, Neves et al., (2018), based on the interpretation of aeromagnetic data and on field and microstructural work, demonstrated that the CNSZ is dextral, constituting a conjugate pair with the sinistral Congo shear zone (Fig. 1). Westward, the CNSZ is partially covered by sedimentary rocks of the Jatobá Basin, but its continuity with the West Pernambuco shear zone can be inferred through the analyses of aeromagnetic data (Fig. 2a). The mylonitic foliation generally strikes ENE-WSW with a dip oscillating from 60° N NW and SSE to subvertical (Figs. 3,4). Mylonitic foliation planes carry a shallow plunging to sub-horizontal (< 30°) stretching lineation defined by elongation of quartz and feldspar (Fig. 3c).

The main protoliths of the mylonites from the CNSZ are: (i) dioritic to granitic orthogneisses (Fig. 4a) related to the Floresta and Cabaceiras complexes, which have been dated at ca. 2.1 Ga (Santos, 1995; Santos et al., 2017) and 2.05 Ga (Neves et al., 2015), respectively; (ii) garnet-bearing, coarse-grained to pegmatitic muscovite granite (Fig. 4b; Neves et al., 2018); and (iii) peralkaline granitoids of the Vila Moderna Intrusive Suite (Fig. 4c; Santos and Vasconcelos, 1973; Santos, 2012). One pluton of this latter suite yielded a U-Pb zircon age of 590 ± 5 Ma (Santos, 2012).

Orthogneiss-derived mylonites are banded, reflecting the compositional heterogeneity of their protoliths (Fig. 4a). Granitic bands probably resulted from the injection of syntectonic melts during the activity of the shear zone. At the boundaries of the CNSZ, banded orthogneiss with flat-lying foliation capped by pegmatite granite with protomylonitic vertical foliation can be observed (Fig. 5ci of Neves et al., 2018), suggesting that these granites were emplaced as thin subhorizontal sheets. Elsewhere, the pegmatite granite was converted into a typical S-C mylonite (Fig. 4b). The Vila Moderna Intrusive Suite consists of elongate bodies (Fig. 3) usually showing marked topographic contrast with the country rocks. Although protomylonitic to mylonitic medium-grained varieties are locally found, these granites are commonly converted to fine-grained ultramylonites (Fig. 4c).

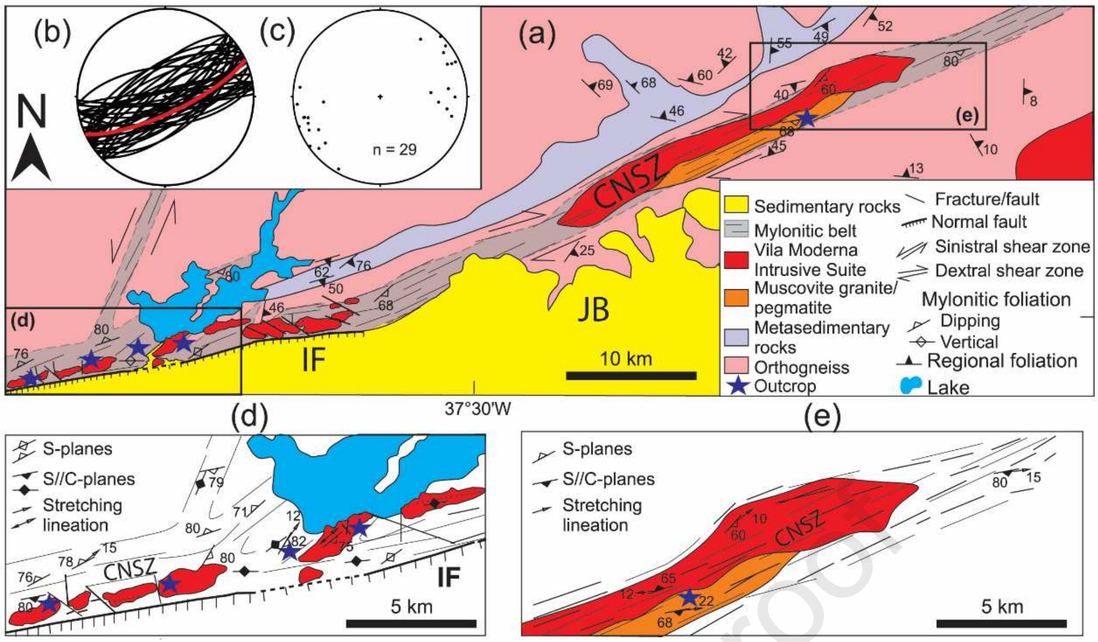

Figure 3. (a) Geological map of the study area. CNSZ, Cruzeiro do Nordeste shear zone; IF, Ibimirim Fault; JB, Jabobá Basin. (b, c) Stereographic projections of mylonitic foliation planes (b) and stretching lineations (c) (Schmidt projections, lower hemisphere). These data represent the average of measured attitudes in all outcrops. Key outcrops are highlighted by the blue stars. (d, e) Enlarged maps of the southwestern (d) and northeastern (e) portions of the CNSZ highlighting the orientation of S and C planes.

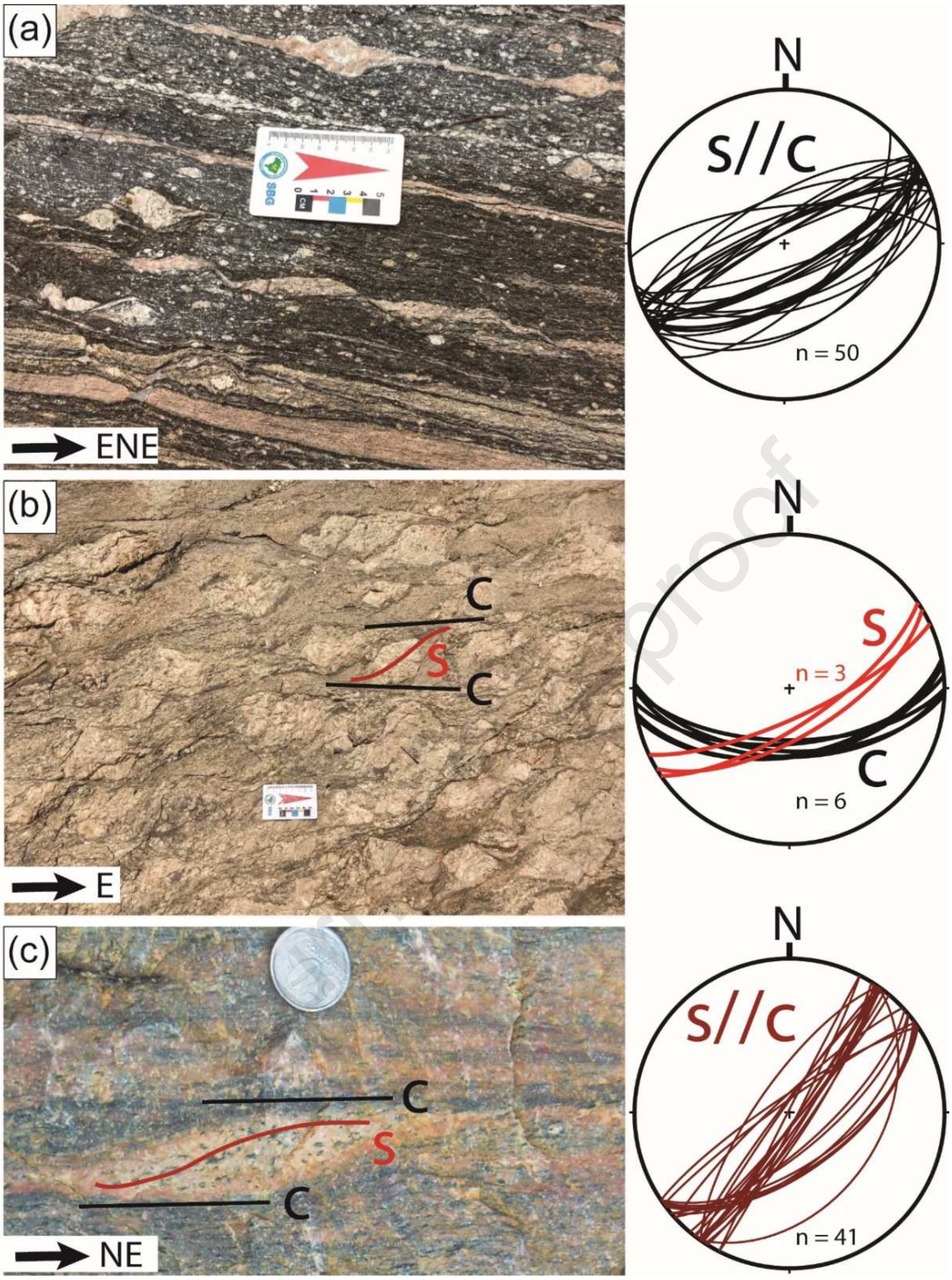

Figure 4. Field aspects of the main protoliths of the CNSZ mylonites and stereographic projections of S and C surfaces measured in the outcrops where photos were taken. All photos are in plan view. (a) Mylonitic banded orthogneiss. Shear band boudins are visible in the granitic band at the center of the photo. (b) Pegmatitic granite with typical S-C fabric. (c) Ultramylonite derived from the granite of the Vila Moderna Intrusive

Suite. A slightly oblique S-surface is preserved in the light and coarser-grained band at the center of the photo. The coin is about 2 cm in diameter.

3.2. Mesoscopic ductile fabrics and kinematic indicators

The mylonitic orthogneisses show a large range of mesoscopic kinematic indicators, which were developed at medium- to high-temperature conditions, as revealed by their microstructures (section 3.5). Almost all shear criteria described in the literature can be found in these rocks and unambiguously indicate dextral shearing. Due to competency contrasts between layers, asymmetric boudins (also called asymmetrical pull-apart or shear band boudins) (e.g., Hanmer, 1986; Goldstein, 1988; Goscombe and Passchier, 2003) are very commonly developed in banded mylonites, particularly affecting amphibolitic and coarse-grained granitic layers (Figs. 4a and 5a). In the latter, feldspar porphyroclasts (e.g., Passchier and Simpson, 1986) with both σ (Fig. 5b) and δ (Fig. 5c) asymmetry are common, as well as synthetic faults in fractured porphyroclasts (Fig. 5d), quartz-feldspar sigmoids (Fig. 5c) and S-C fabrics (e.g., Lister and Snoke, 1984; Fig. 5b). C'-type shear bands (e.g., Blenkinsop and Treloar, 1995) cutting across the composite S-C fabric are also common (Fig. 5b). These shear bands can be distinguished from those developed at the brittle-ductile transition (section 3.3) because they show drag folds associated to the shear planes, commonly make a smaller angle (10-20°) with the main mylonitic foliation, and lack evidence of brittle fracturing at the mesoscopic scale. Inhomogeneous flow revealed by development of synmylonitic folds with Z asymmetric is also locally recorded (Fig. 5c of Neves et al., 2018).

C and C'-type shear bands are the most conspicuous shear criteria in the pegmatitic granite (Figs. 4b, 5e, 5f). The ductile behavior of the large K-feldspar megacrysts in the pegmatitic bands, which are converted to augens, indicates deformation at high temperature. The shape preferred orientation of these porphyroclasts defines the S surfaces, which make angles ranging from c. 40º to 20º with the C surfaces defined by quartz ribbons up to 1 cm wide (Fig. 5f). In the equigranular portions, S and C are subparallel. C'-type shear bands display brittle-ductile behavior and are described in section 3.3.

The granites of the Vila Moderna Intrusive Suite were converted to ultramylonites and the typical fine grain size suggests deformation at lower temperature conditions than in the mylonitic orthogneiss and granite pegmatite. Shear criteria are rarely observed, but decimeter-long shear bands (Fig. 5h) S-C fabrics in coarser-grained varieties (Fig. 5g) and indicate dextral shearing.

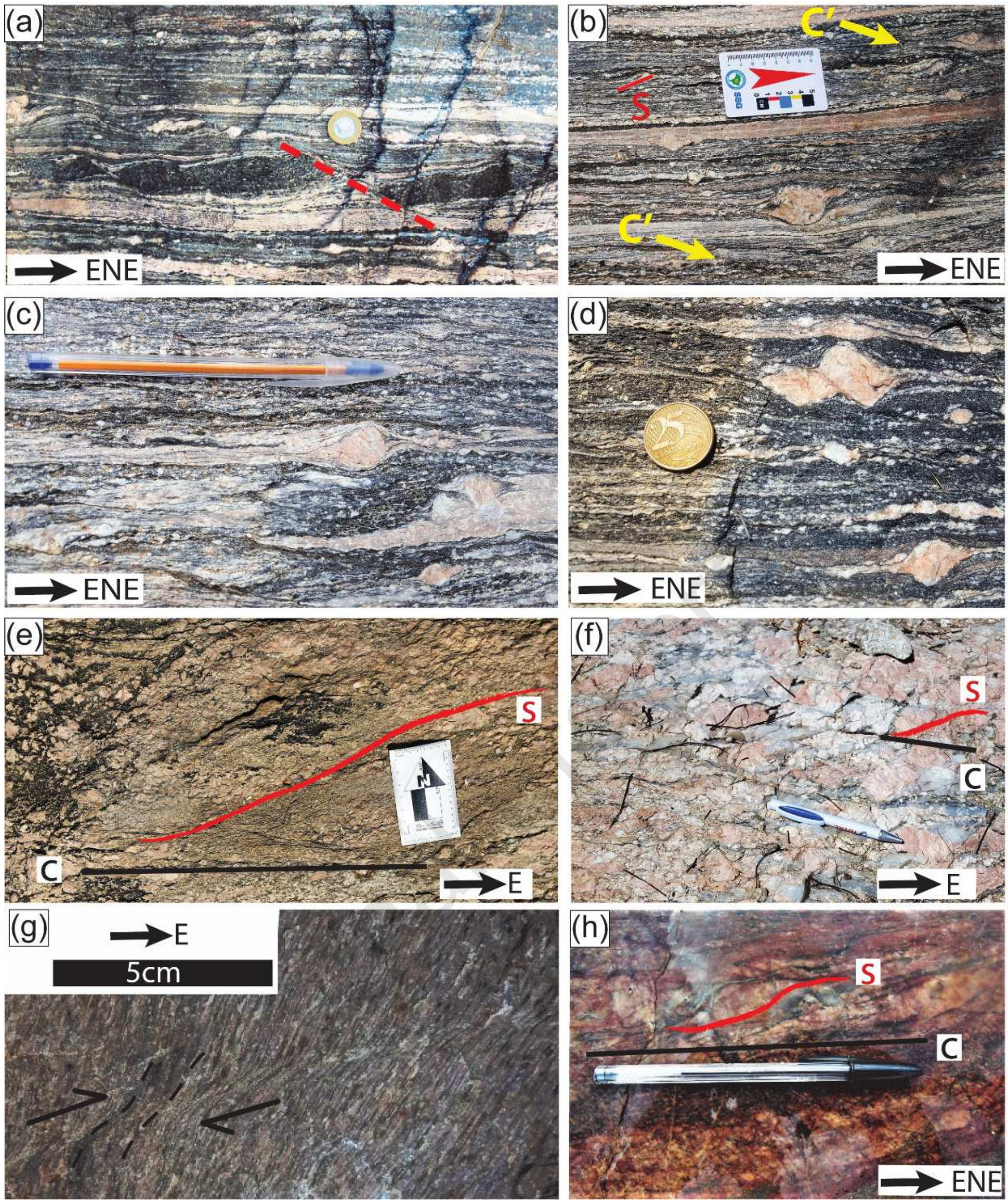

Figure 5. Shear criteria in mylonitic orthogneiss (a-d), pegmatite granite (e, f) and granitoids of the Vila Moderna Intrusive Suite (g, h). All photos were taken on surfaces perpendicular to the mylonitic foliation and parallel to the stretching lineation (sub-horizontal planes). (a) Shear band boudins in the amphibolitic layer. (b) Large σ-type porphyroclast. C'-type shear bands (indicated by arrows) are visible at lower left and upper right and S-C fabric to the left of the scale. (c) δ-type (center) and σ–type (lower right) porphyroclasts and quartz-feldspar sigmoid (right). (d) Synthetic fault in

porphyroclast. (e, f,) S-C fabric. Note the large width of quartz ribbons defining the C surfaces in (f). (g) Shear band. (h) S-C fabric. The coin is about 2 cm in diameter.

3.3. Ductile to brittle fabrics

The mylonites from the CNSZ are crosscut by C’-type shear bands that strike E-W and usually make angles of 20 to 40º with the main foliation. They are straighter and longer than those described in section 3.2 and may evolve to brittle faults. In orthogneiss protoliths, the S-C foliation may show from marked to only slight curvature toward the shear bands (Figs. 6a, b). In the first case, the central deformed portion is a very fine-grained ultramylonite whereas in the other case it may show brittle deformation (Fig. 6b). This latter situation predominates in the pegmatite granite (Fig. 6c) and in granites of the Vila Moderna Suite (Fig. 6d).

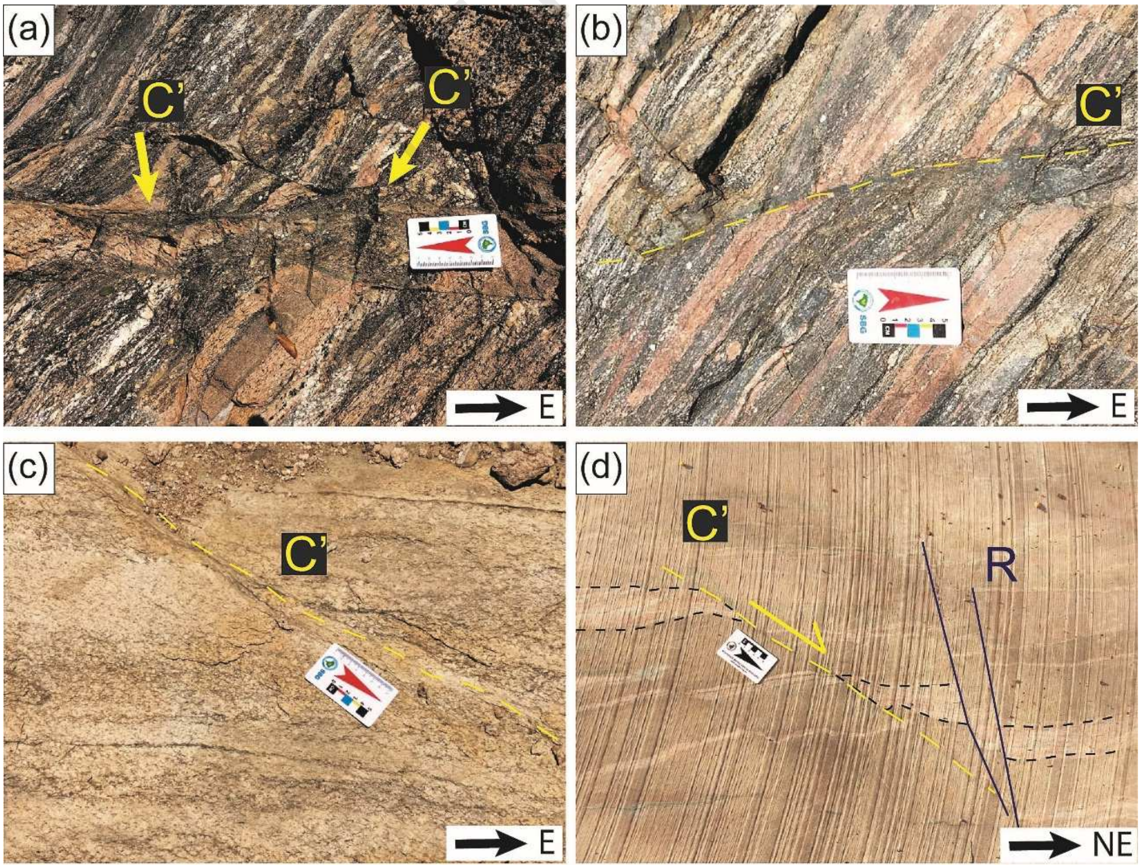

Figure 6. Brittle-ductile C'-type shear bands in mylonitic orthogneiss (a, b), pegmatite granite (c) and granite from the Vila Moderna Intrusive Suite (d). All photos are in the plan view. The striated surface in (d) resulted from the extraction of blocks to produce ornamental stones, which masks the deflection of the mylonitic foliation towards the shear bands. The central shear band and the displaced markers are highlighted by the yellow (arrows) and black lines, respectively, both of which being crosscut by an R shear (blue line). Several other smaller shear fractures (e.g., R synthetic fault) that merge with C' are also visible.

WNW-ESE and N-S strike-slip faults, dextral and sinistral, respectively, represent the most prominent brittle-ductile structures in the study area (Figs. 7 and 8). They show displacements that range from 1 to 4 cm and display a sinuous shape, which makes an oblique orientation in relation to the SC foliation. The curvature of the mylonitic foliation toward the faults indicates that deformation started in the ductile field (Figs. 7 and 8). The sense of shear is evidenced in plan view by displaced markers and on fault planes by very strong horizontal slickenfibres and steps that are marked by epidote and calcite (Fig. 7 e,f). These structures are interpreted as the R (WNW-ESE) and R' (N-S) faults of the Riedel system (e.g., MacClay, 1987; Fig. 8). This conjugate pair is associated with C' shear bands, which can be interpreted as representing the principal displacement zone (PDZ or Y-shear) that strikes N85W (Fig. 8a, e). The synthetic fault (R) is oriented ~15° (clockwise) from the PDZ. R' shears strike N10W and make ~75° with the PDZ (Fig. 8d). . Tension gashes, which represent the T-fractures, striking NW-SE, as high-angle dipping veins, are localized on the bisectrix of the strike-slip fault conjugate pair (Fig. 8b,e. R, R', PDZ and T structures are arranged in an en echelon array, which is postulated as one of the chief characteristics of a Riedel shear system (e.g., Davis et al., 2000). This Riedel structure geometry is consistent with the dextral sense of shear that is correlated to the ductile deformation of the CNSZ.

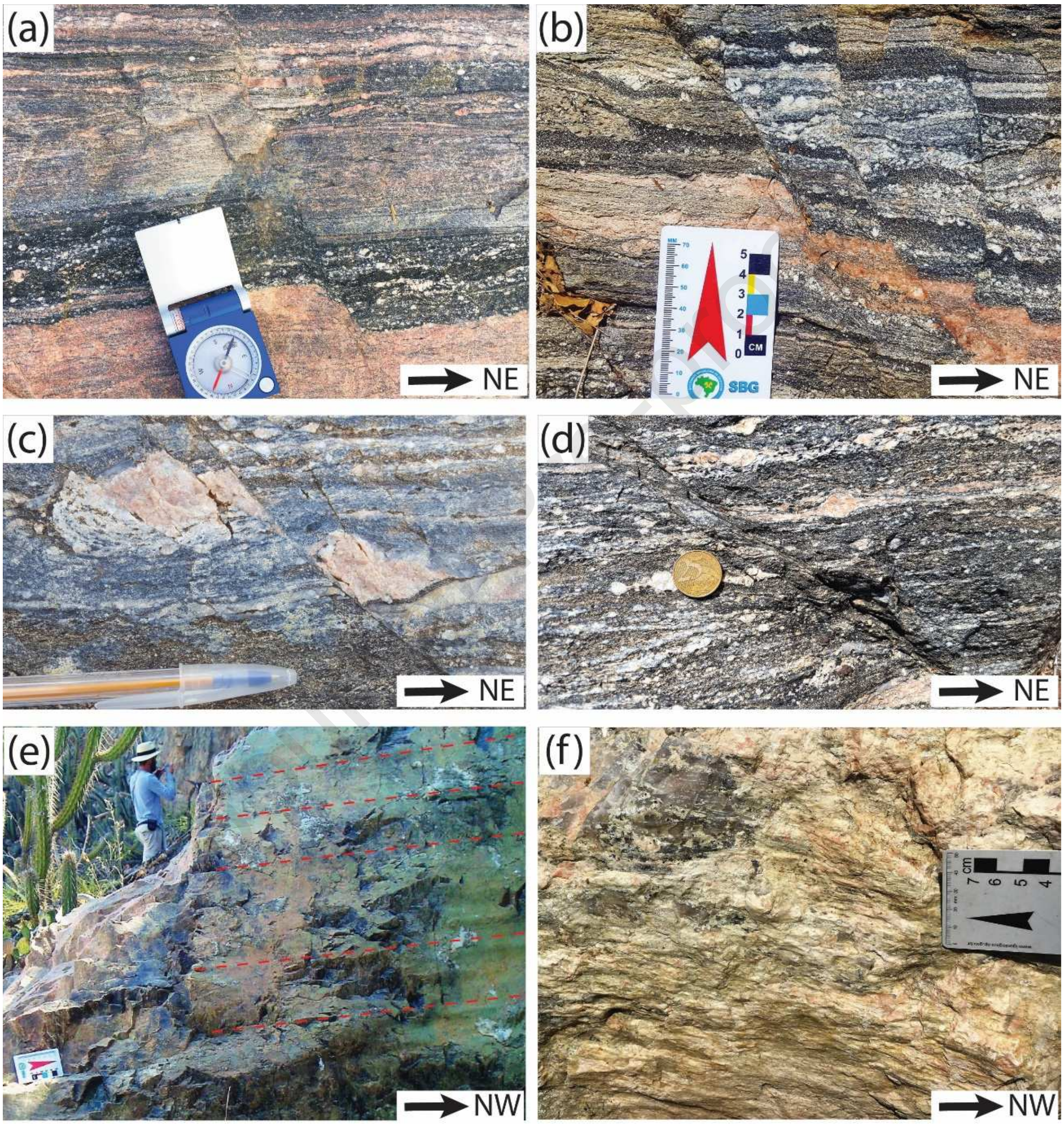

Figure 7. (a-d) Dextral strike-slip faults in mylonitic orthogneiss. Note the curvature of the mylonitic foliation towards the shear fractures. Photographs were taken on surfaces perpendicular to the mylonitic foliation and parallel to the slickenlines (plan view). The coin is about 2 cm in diameter. (e) WNW-ESE-striking fault surface in the Vila Moderna Intrusive Suite, showing subhorizontal slickenfibres striations marked by

epidote (red dashed lines) and associated with calcite slikenfibers. (f) Slip surface in pegmatite granite displaying steps and horizontal quartz slickenfibres.

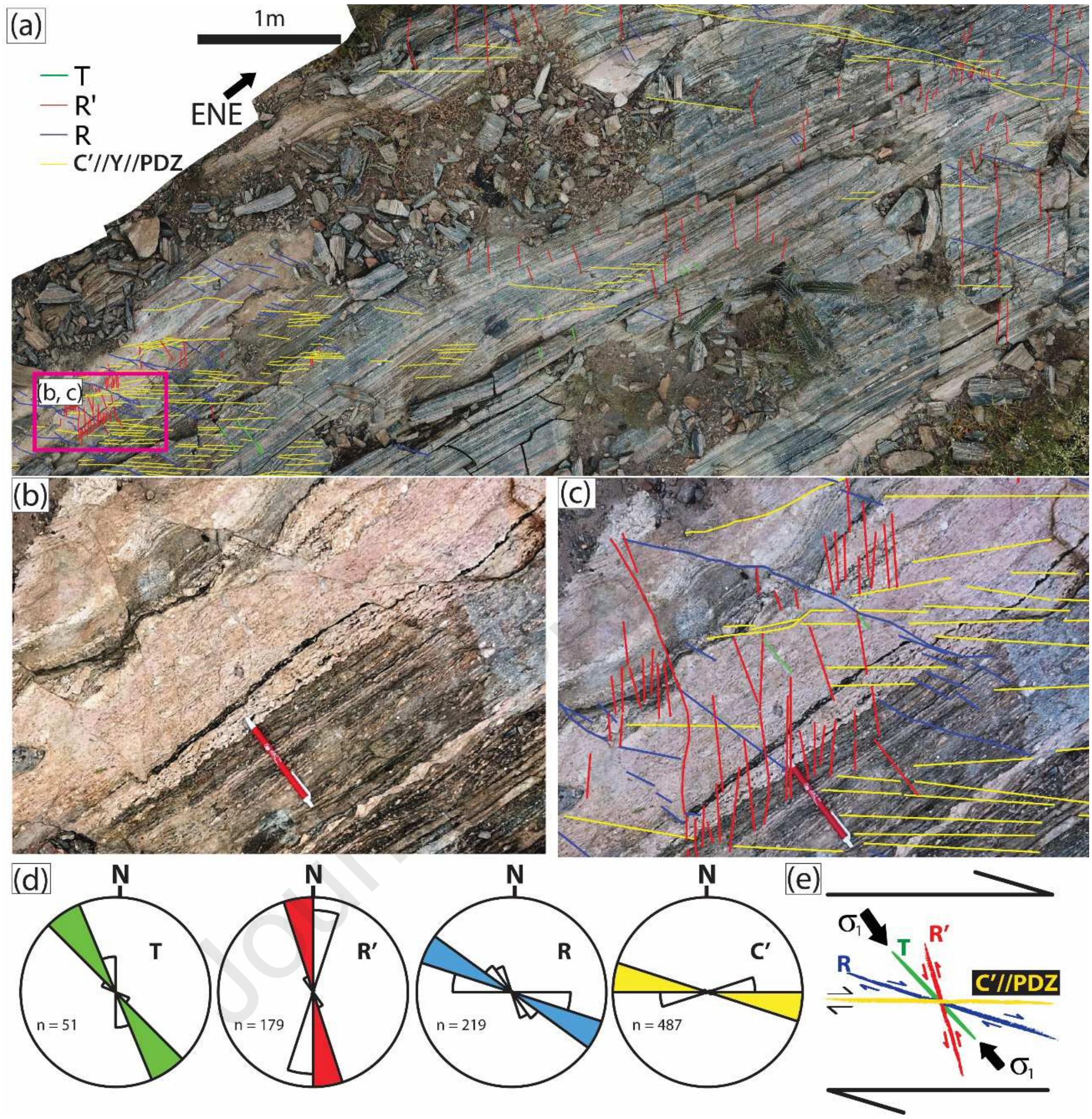

Figure 8. (a) Orthophotograph (resulting from drone imagery) in the plan view of the mylonitic banded orthogneiss showing conjugate pairs of strike-slip faults (red and blue) and C' shear bands (yellow). (b, c) Detail showing conjugate pair of strike-slip faults (R, dextral; and R', sinistral) superimposed to the SC foliation, which shows a slight sinuosity indicating development of the shear fractures during the ductile-brittle transition. Tension gashes (T vein) are located on the bisectrix of the acute angle of the R and R'. (d) Rose diagrams of the T, R', R and C' shear bands. (e) C' shear bands

interpreted as parallel to the principal displacement zone (PDZ or Y) in the Riedel model, with the maximum compressive stress axes-oriented NW-SE, consistent with the dextral sense of shear.

3.4.Brittle deformation

The SC foliation of the CNSZ is overprinted by a system of normal faults filled by calcite, which show a predominantly NE-SW orientation, with a pole maximum at 130/05 (Fig. 9). The normal faults display striated slip surfaces showing down-dip slickenfibres marked by calcite. These faults can be distinguished from those developed at the brittle-ductile transition because they are parallel to the main mylonitic foliation and do not show evidence of ductile deformation and epidote mineralization in the fault plane at the mesoscopic scale. Thus, this brittle deformation can be linked to the Ibimirim Fault zone (ENE-WSW), which is parallel to the mylonitic foliation and marks the northern border of the Jatobá Basin (Fig. 3). Moreover, calcite is commonly found filling the slip surfaces as slickenfibres (Fig. 9). This is consistent with a brittle reactivation of the SC foliation, and possibly related to hydrothermal processes. Brittle reactivation of R and R' shears were also observed in the Vila Moderna Intrusive Suite (Fig. 10). As a result, several fault rocks, such as breccia, cataclasite and gouge were formed at their cores (Fig. 10). The fault breccia comprises mylonitic angular fragments (> 1 cm) and its width range from 1 cm to 1m (Fig. 10b). The breccia shows different types of textures, concentration, and rotation of their fragments, which are possibly formed by the infilling of hydrothermal minerals (e.g., calcite) (e.g., Woodcock and Mort, 2008).

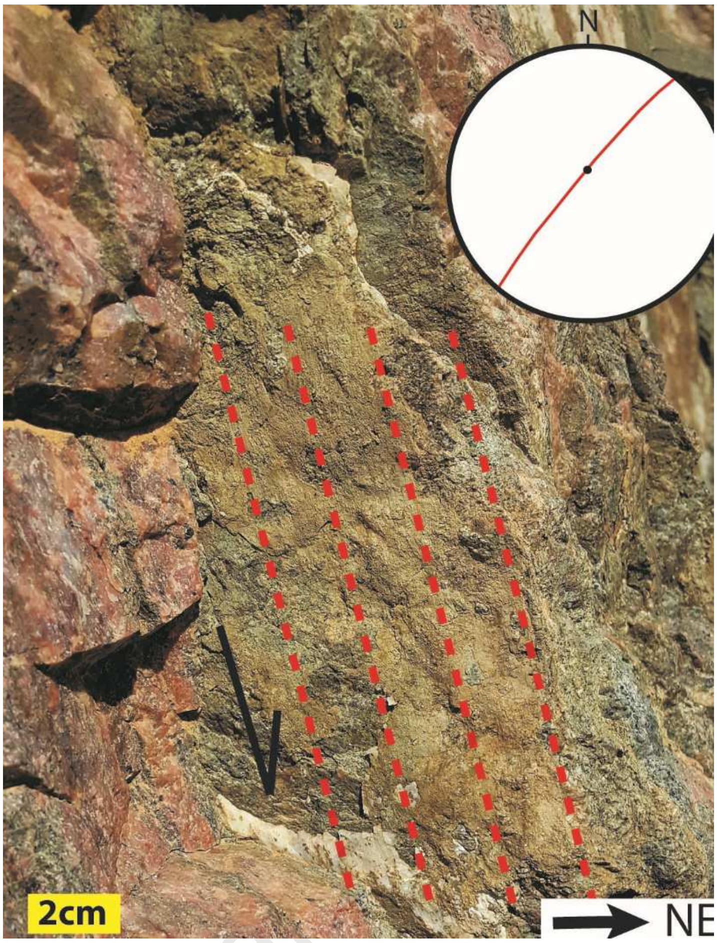

Figure 9. Brittle reactivation of the SC foliation plane as NE-SW striking normal fault bearing high-rake slickenfibres. Note that the slickenfibres are composed of calcite (red dashed line) (Vila Moderna Intrusive Suite). The inset shows stereograph projection (lower hemisphere) of the normal fault showing the down-dip striation (black dot).

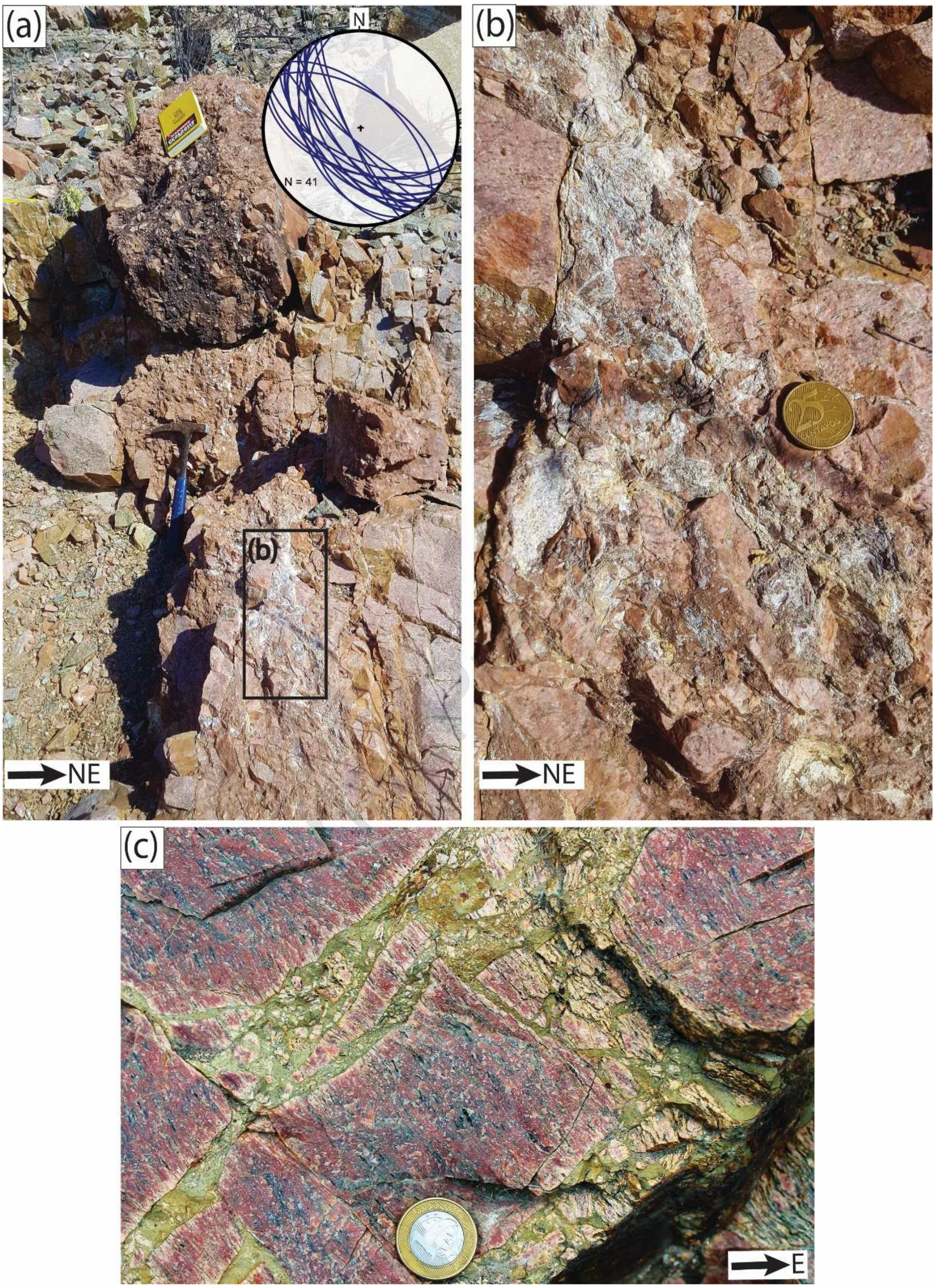

Figure 10. Fault rocks related to dextral NW-SE strike-slip faults from the Vila Moderna Intrusive Suite. (a) Cataclasite and fault breccia showing mylonitic angular fragments and calcite cement. The inset shows stereograph projection (lower

hemisphere) of the R strike-slip fault. (b) Fault breccia cemented by calcite. The coin is about 2 cm in diameter. (c) Fault breccia filled by epidote.

3.5. Microstructures

3.5.1. Evidence for transition from crystal plastic- to brittle deformation mechanisms

The ductile to brittle transition observed at the mesoscopic scale is also recorded by microstructures indicating their continuous development at declining temperature conditions. High-temperature fabrics superimposed by medium- to low-temperature fabrics and then by microfaults are particularly well-displayed by orthogneiss-derived mylonites (Fig. 11). The main microstructural type of these rocks is an S-C fabric consisting of large quartz ribbons and biotite flakes defining the C surfaces, and porphyroclasts of K-feldspar and plagioclase, inclined at angles of 0-30º in a dextral sense to the C shear bands, defining the S-planes (Figs. 11a). Feldspars show dynamic recrystallization by subgrain rotation recrystallization and myrmekite is abundant at the contact of K-feldspar porphyroclasts with plagioclase, with their asymmetric distribution (quarter structure; Hanmer and Passchier, 1991) indicating clockwise shearing (Fig. 11a). Quartz ribbons show dynamic recrystallization dominantly by grain boundary migration, with coarse subgrains (100-200 μm) showing interlobate and ameboid contacts (Fig. 11b). These microstructures indicate that the development of the S-C fabric started at high temperature conditions (> 550°C) (Olsen and Kohstedt, 1985; Simpson and Wintsch, 1989; Miller and Paterson, 1994; Stipp et al., 2002; Mainprice et al., 1986). Finer grained quartz-feldspar aggregates where quartz recrystallizes by subgrain rotation (Fig. 12c, d) is also common and denotes deformation at a somewhat lower temperature.

Discreet C'-type shear bands cutting at a low angle the C surfaces are characterized by their fine grain size (Fig. 11d) but quartz recrystallization is still dominantly by subgrain rotation. Microstructures that record low temperature crystal plastic deformation are marked by C'-type shear bands cutting at a high angle the mylonitic foliation, bulging recrystallization of quartz, and fractured feldspar grains (Figs. 11e-h). The shear bands show clear dextral kinematics and a marked reduction in grain size. Usually they are < 0.5 mm thick (Fig. 12e) but locally may reach up to 4 mm (Figs. 12f). At still lower temperatures, microfaults with dextral kinematics displace biotite layers and quartz ribbons (Figs. 11g, h). These layers are rotated towards the microfaults indicating development at the brittle-ductile transition (c. 300°C).

Like the mylonitic orthogneiss, the finer grained portions of the mylonitic muscovite granite display an S-C fabric, with anastomosed quartz ribbons both parallel to C-planes and wrapping around plagioclase and K-feldspar porphyroclasts (Fig. 12a). However, here the most conspicuous feature is the presence of mica-fish of muscovite. Mica fishes may show several morphologies (e.g., ten Grotenhuis et al., 2003; Mukherjee, 2011), the most common in the present case being lenticular, sigmoid and rhomboidal ones (Figs. 12a-d) . The microstructure records deformation under continuous declining temperature (e.g., Stipp et al., 2002). At the high temperature end, quartz ribbons show dynamic recrystallization by grain boundary migration (Fig. 12b), myrmekite develops around K-feldspar porphyroclasts, and both feldspars may show a mantle of neoformed grains resulting from subgrain rotation recrystallization. More commonly, quartz recrystallizes by subgrain rotation, indicating deformation at moderate temperature (c. 400-500 ºC), and the new grains display oblique shape preferred orientation indicating dextral shear sense (Fig. 12a). Deformation at a lower temperature is recorded in C planes and C'-type shear bands that are defined by trails of very fine-grained quartz and muscovite (Fig. 12d). Much of the fracturing observed in some feldspar porphyroclasts probably formed at this late stage of deformation.

Granitic bands intercalated with the mylonitic orthogneiss and mylonitic granitoids from the Vila Moderna Intrusive Suite show similar microstructural characteristics. Both display advanced recrystallization, with a few remnant porphyroclasts involved by a quartz-feldspar matrix. Shear criteria are less conspicuous than in the mylonitic orthogneiss. The quartz-feldspar aggregates display only a weak preferred orientation that is subparallel to C shear bands defined by biotite (Fig. 13a), indicating rotation of S planes towards the shear plane. In the case of the Vila Moderna Intrusive Suite, retrogression of amphibole to fibrous actinolite along its margins defines asymmetric structures (Fig. 13b). The ductile-brittle transition is characterized by the development of very fine-grained C'-type shear bands that usually make angles of 25-40° to the main foliation (Fig. 13c) and extreme cataclasis of feldspar porphyroclasts (Fig. 13d).The microstructural modifications are accompanied by retrogression of plagioclase to aggregates of epidote and calcite and of amphibole to epidote and/or chlorite. Some fractures lack shear displacement and have the same orientation of tension gashes observed at the mesoscopic scale, suggesting they correspond to T fractures (cf. Fig. 8).

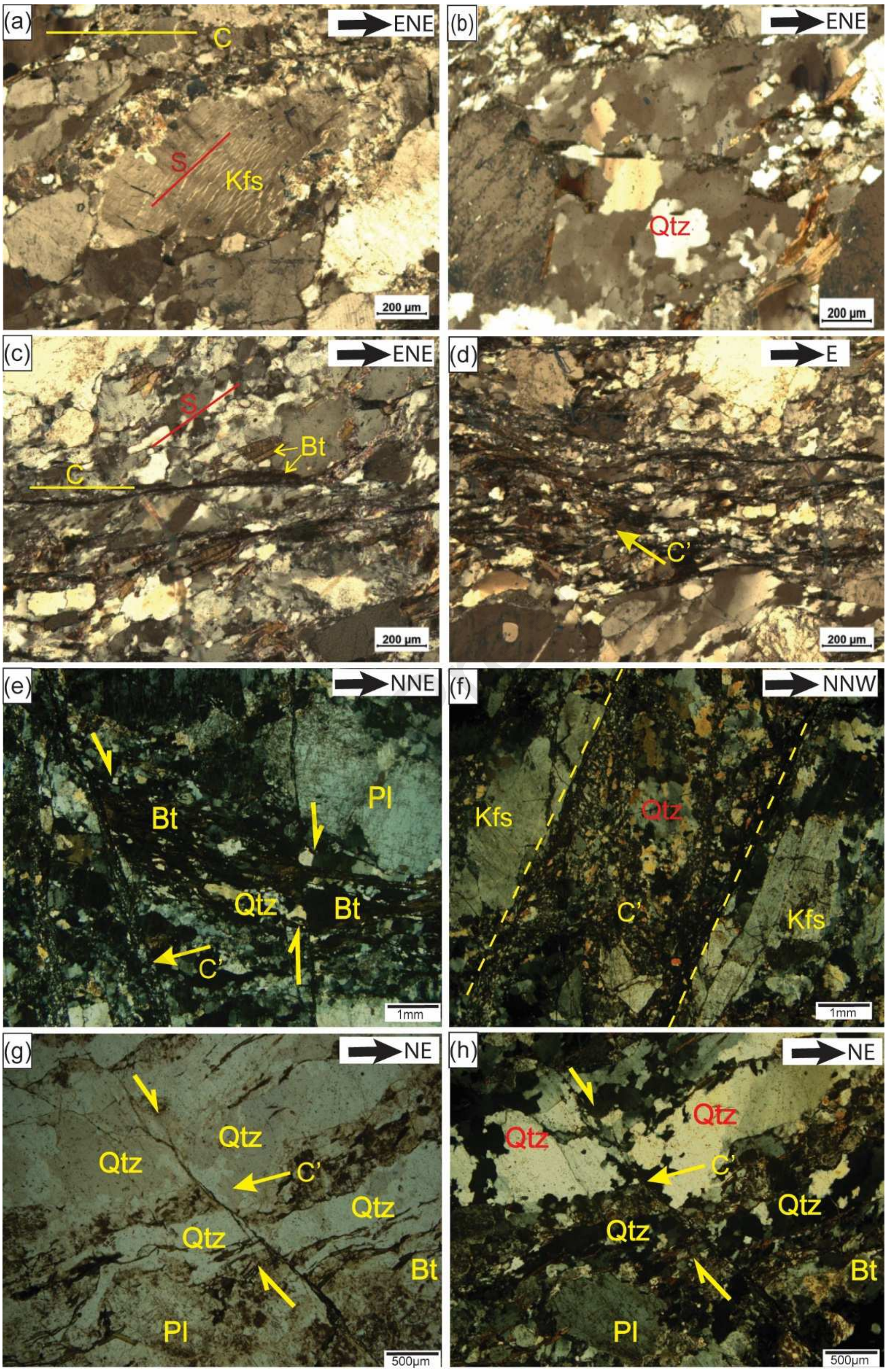

Figure 11. Microstructural aspects of mylonite orthogneiss from the CNSZ. Sections are perpendicular to mylonitic foliation and parallel to stretching lineation. All photomicrographs are in crossed polarized light (CPL), except (g) that was taken in

parallel polarized light (PPL). (a, b) High-temperature microstructural features. (a) Microperthitic K-feldspar with asymmetric dynamically recrystallized tails with long axes oblique to C-planes. (b) Large quartz ribbon showing interlobate and ameboid subgrain boundaries indicating dynamic recrystallization by grain boundary migration. (c, d) Moderate-temperature microstructural features. (c) S-C fabric where fine-grained quartz-feldspar aggregates are separated by C planes defined by biotite. (d) C'-type shear band. (e-h) Low-temperature microstructural features. (e) Shear band is defined by fine-grained biotite and quartz suggesting recrystallization by bulging. (f) Thick shear band (center of the image) filled with recrystallized material, surrounded by two intensely fractured K-feldspar grains. (g, h) Microfault displacing quartz ribbons that curve towards the fault. Mineral abbreviations: Qtz, quartz; Kfs, K-feldspar; Pl, plagioclase, Bt, biotite.

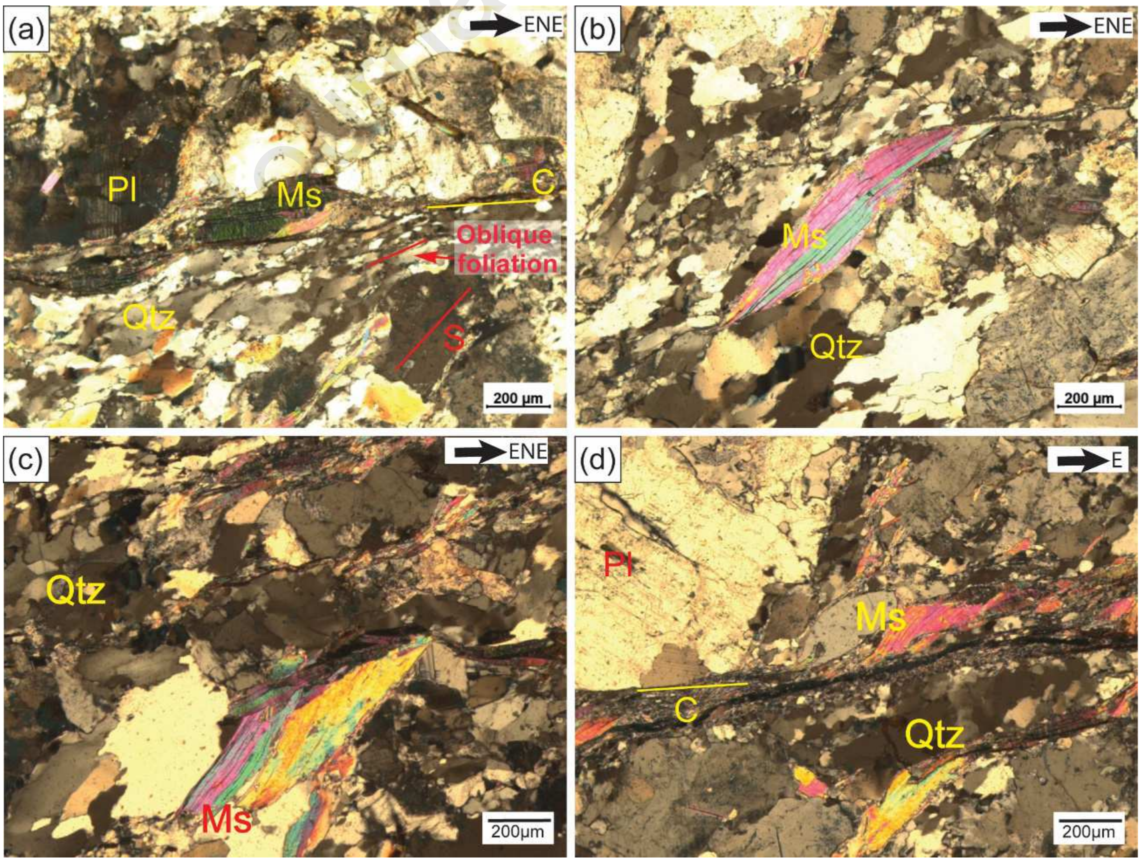

Fig. 12. (a-d) Microstructural aspects of mylonitic muscovite granite. Sections are perpendicular to mylonitic foliation and parallel to stretching lineation. All photomicrographs in CPL. (a) S-C fabric with elongate muscovite fish along C-plane. Quartz ribbon shows recrystallization by subgrain rotation and oblique foliation. (b) Lenticular micafish. Quartz shows interlobate subgrain boundaries suggesting dynamic recrystallization by grain boundary migration. (c) Rhomboidal muscovite fish. (d) C shear band is defined by finely recrystallized quartz and muscovite. Note the fractured plagioclase porphyroclast and the lenticular muscovite fish. Mineral abbreviations: Qtz, quartz; Pl, plagioclase; Ms, muscovite.

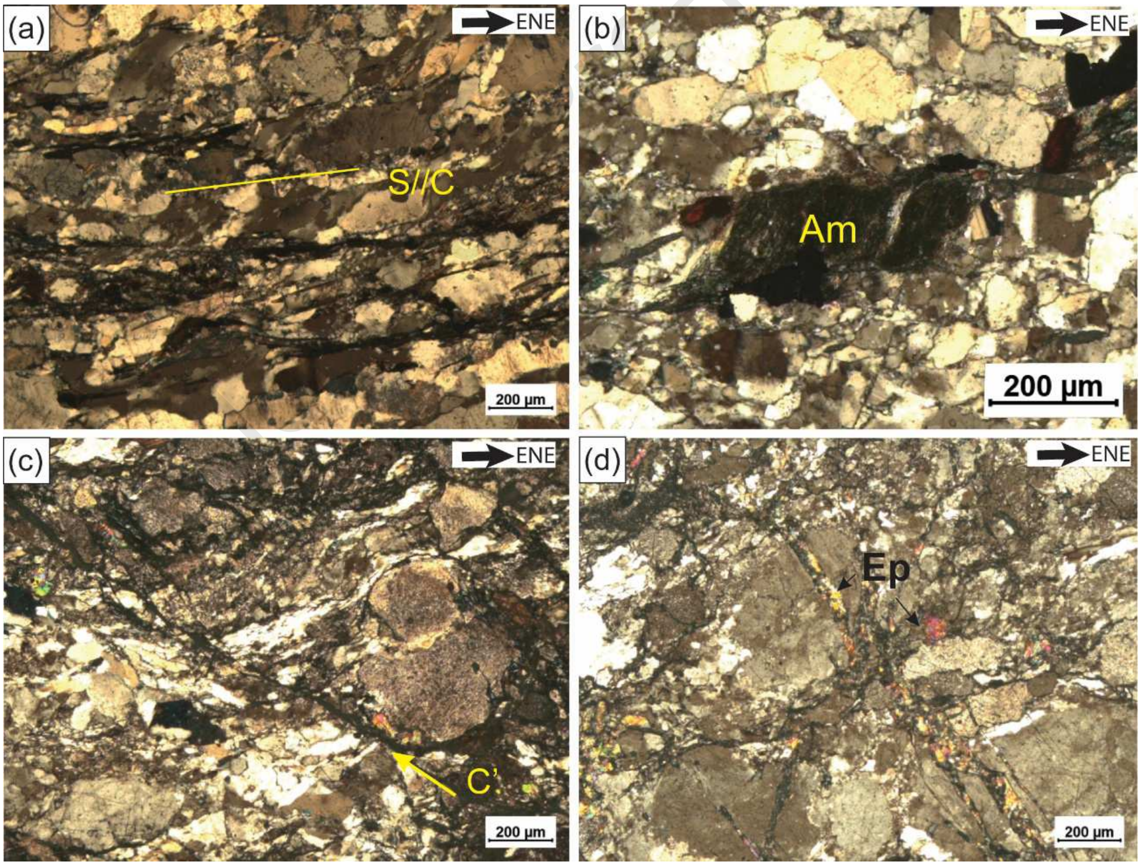

Fig. 13. Microstructural aspects of mylonites from Vila Moderna Intrusive Suite. Sections are perpendicular to mylonitic foliation and parallel to stretching lineation. All photomicrographs in CPL. (a) Main foliation with S//C fabric. (b) Prismatic amphibole

with recrystallized asymmetric tails of actinolite. (c) Brittle-ductile C'-type shear band. (d) Cataclastic mylonite crosscut at a high angle by extension fracture filled with epidote. Mineral abbreviations: Amp, amphibole; Ep, epidote, Qtz, quartz.

3.5.2. Brittle deformation

Microstructures that record brittle reactivation of the CNSZ associated with R-synthetic faults, which was dated in this work (see section 4), are evidenced by the occurrence of calcite slickenfibres within the fault core. The active deformation mechanism is cataclasis, which can significantly alter the original properties of the host rock (Fig. 14).

Figure 14 illustrates a profile across a calcite slickenfibres. Along this profile four consecutive domains are observed: vein, ultracataclasite, cataclasite and host rock. The slickenfibre domain is composed of well-developed calcite with coarse granulation. Immersed in this material occur scattered fragments of the host rock, which are angular and of varying sizes. The domain composed of ultracataclasite is characterized by two sectors: a) matrix; b) porphyroclasts. The matrix is very thin and composed of calcite and quartz-feldspathic fragments; the porphyroclasts are angular monomineralic and rock fragments occur immersed in this matrix with varying sizes. The cataclasite domain is marked by the presence of calcite-filled veins that crosscut the host rock, giving the cataclasis texture, which does not show observable rotation. The last domain comprises the host rock, which is dominated by lower deformation intensity characterized by minimal frequency of fractures. From this analysis, starting from the vein to the host rock, it is possible to observe an increase of deformation near the slickenfibres, characterized by the occurrence of fault rocks (ultracataclasite and cataclasite) and a decrease in the degree of deformation as it moves to the host rock.

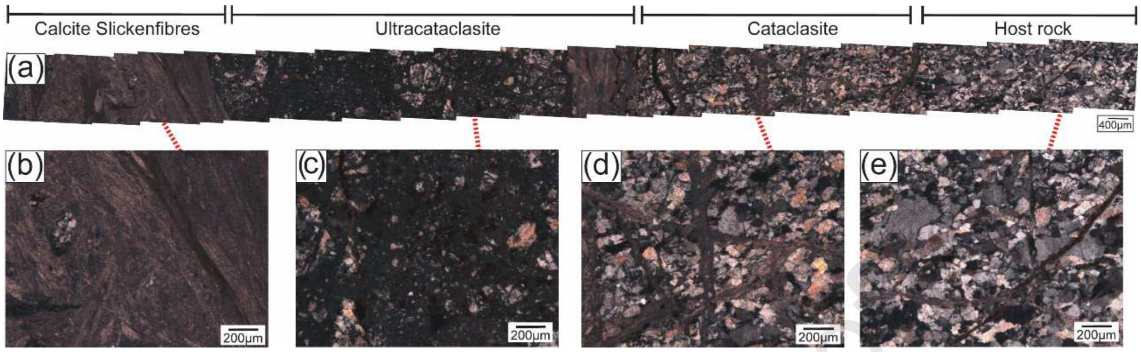

Figure 14. (a) Profile across a WNW-ESE trending strike-slip fault zone that contains calcite slickenfibres from the Vila Moderna Intrusive Suite. From left to right: (b) calcite slickenfibres, (c) ultracataclasite. (d) cataclasite, and (e) host rock.

4. Timing of brittle reactivation of the Cruzeiro do Nordeste shear zone

To constrain the timing of brittle reactivation of the Cruzeiro do Nordeste shear zone, we dated synkinematic slickenfibre calcite using U-Pb geochronology from a well exposed dextral strike-slip fault striking WNW-ESE from the Vila Moderna Intrusive suite (Fig. 15). Two samples comprising slickenfibre calcite were taken from the same outcropping fault plane and were cast into polished blocks for analysis. Both samples (PC1_a and PC1_b) exhibit complex textures, dominated by roughly 0.5 to 1 mm thick calcite plates stacked into several mm-thick sets of slickenfibers. PC1_b shows disturbance of the slickenfire by later fault movement and fluid infiltration (marked by a separate cement). Along with the multiple packages of slickenfibres, the microstructures indicate protracted periods of crack-seal-slip type fault movement, interspersed by periods where the orientation changes such that a break in slickenfibre growth occurs.

Both samples were analyzed using Laser Ablation Inductively Coupled Mass Spectometry (LA-ICP-MS) U-Pb geochronology at the British Geological Survey (UK), using the method described in Roberts et al. (2017). See supplementary files for a full description of the method and the full dataset. Three regions across the two samples were dated, two from the opposing outside edges of PC1_a and one from the central region of PC1_b; all were within uncertainty of each other (135.3 ± 2.6, 136.7 ± 5.4 and 134 ± 17 Ma, 2σ). The data indicate that although the textures indicate a possible protracted history of fault slip, the timing of fault movement was probably constrained to a period of a few million years at maximum. Pooling all the data into a single result provides an estimated timing of fault slip of 134.5 ± 4.7 Ma (2σ) (Fig. 16).

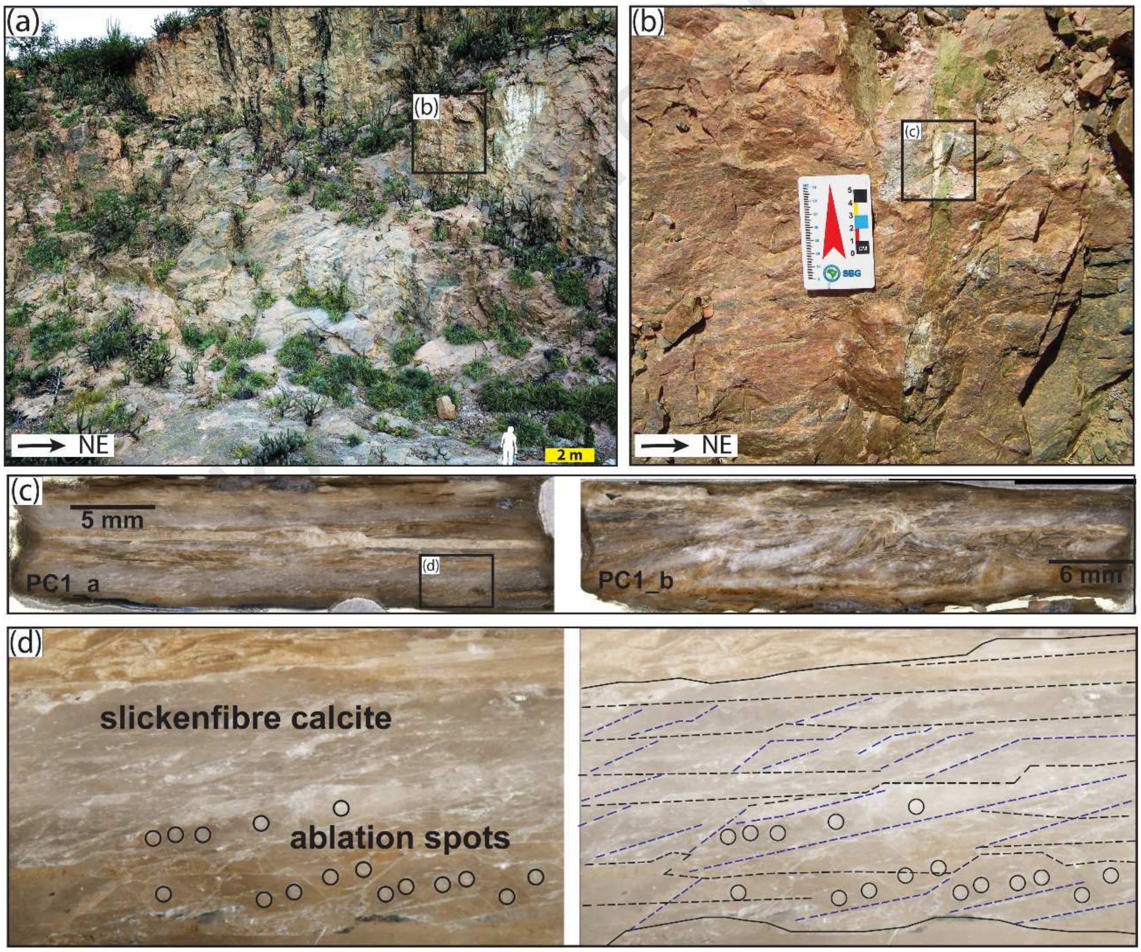

Figure 15. (a) General view of Vila Moderna Intrusive Suite outcrop where samples for U-Pb dating were collected. (b) WNW-ESE, dextral, strike-slip fault core filled by

calcite. Photographs of dated samples (c) and (d) and slickenfibre calcite, with ablation spots, interpreted slip planes (black) and calcite crystal boundaries (blue) below.

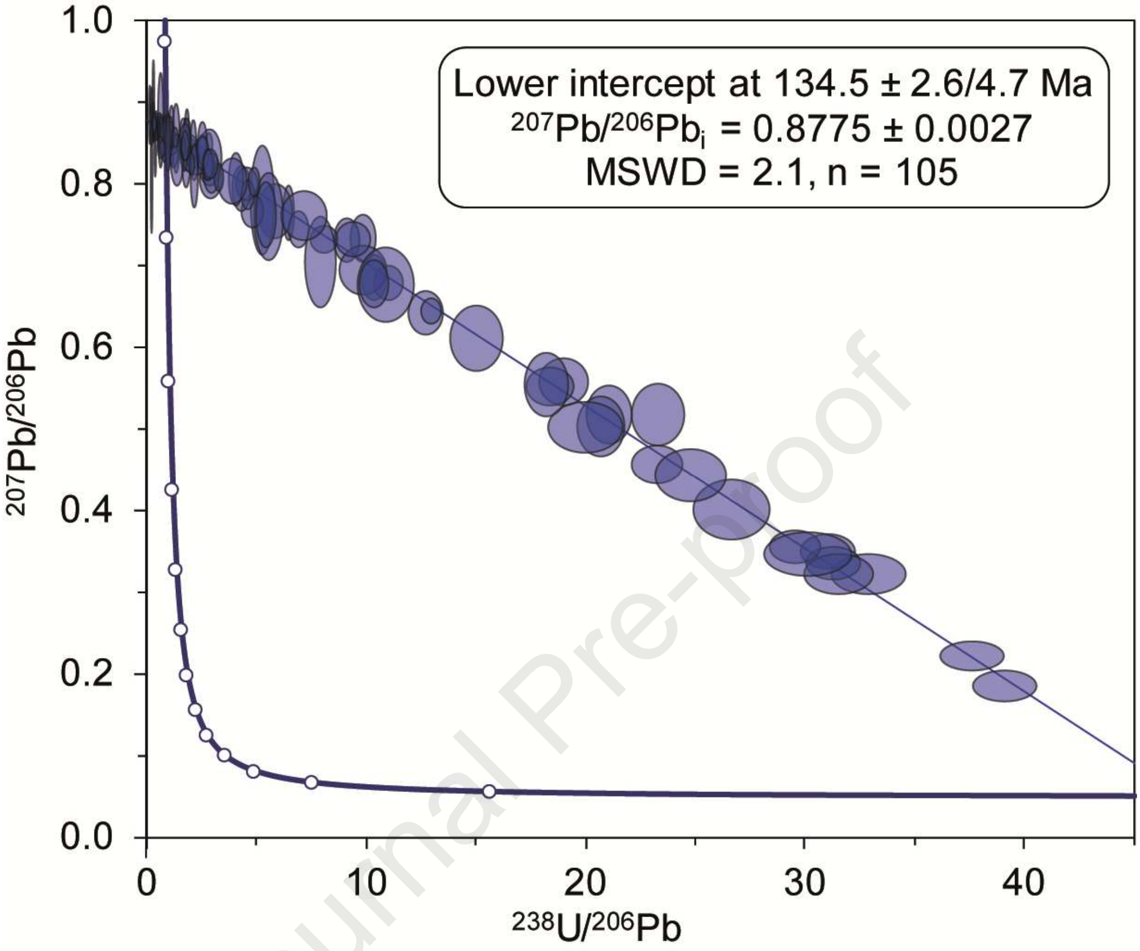

Figure 16. Tera-Wasserburg Concordia plot showing U-Pb date for combined PC1_a and PC1_b data from the NW-SE trending strike-slip fault of the Vila Moderna Intrusive Suite.

5. Discussion

The Borborema Province is a key region to understand the cooler semi-brittle to brittle deformation superimposed on ductile fabrics as it contains a vast number of continental-scale shear zones that border intraplate sedimentary basins. In the previous sections, we (i) presented evidence from the CNSZ for a transition from high temperature to low temperature ductile fabrics and then to brittle fabrics, (ii) analyzed the brittle-ductile transition, and (iii) dated the age of a strike-slip fault that is related to the brittle reactivation of the CNSZ during the Cretaceous. The orientation, spatial distribution and crosscutting relationship between ductile and brittle structures recorded in the study area have significant tectonic implications for the duration of the Brasiliano Orogeny, formation of intraplate basins, and rift systems evolution, which are discussed below.

5.1. Ductile to brittle-ductile transition of the Brasiliano Orogeny

At the macroscale, the E- to NE-trend of magnetic lineaments (Fig. 2a-c) in the Central Subprovince mimics the orientation of dextral and sinistral shear zones, respectively (Fig. 1). The same holds true for the dominant trends of topographic lineaments observed in the digital elevation model (Fig. 2e-h). Because, in the ductile field, the bulk shortening direction bisects the obtuse angle between conjugate shear zones (e.g., Ramsay and Huber, 1987; Carreras et al., 2010; Angen et al., 2014), the orientation of conjugate shear zones with opposed kinematics indicates NW-SE bulk shortening (see also Neves et al., 2018), implying an approximate NW-SE direction of the main compressive stress axis (σ1).

In the digital elevation model (Fig. 2e-h), in addition to the dominant E and NE trends, two subordinate ones, are also observed: N-S and WNW-ESE. If it is assumed that these orientations correspond to the directions of conjugate Andersonian faults with sinistral and dextral kinematics, respectively, a NW trend of σ1 can also be inferred. This would be consistent with the same stress field responsible for development of the ductile fabrics (Fig. 17). In the next paragraphs, we summarize meso- and microscale observations supporting that the ductile and brittle-ductile structures of the CNSZ were formed under the same stress field, with σ1 oriented NW-SE and σ3 NE-SW Fig. 17 is an attempt to show how deformation at declining temperature conditions relates to progressive exhumation, and proposes a kinematic evolution model for the CNSZ and its reactivation during the Cretaceous. .

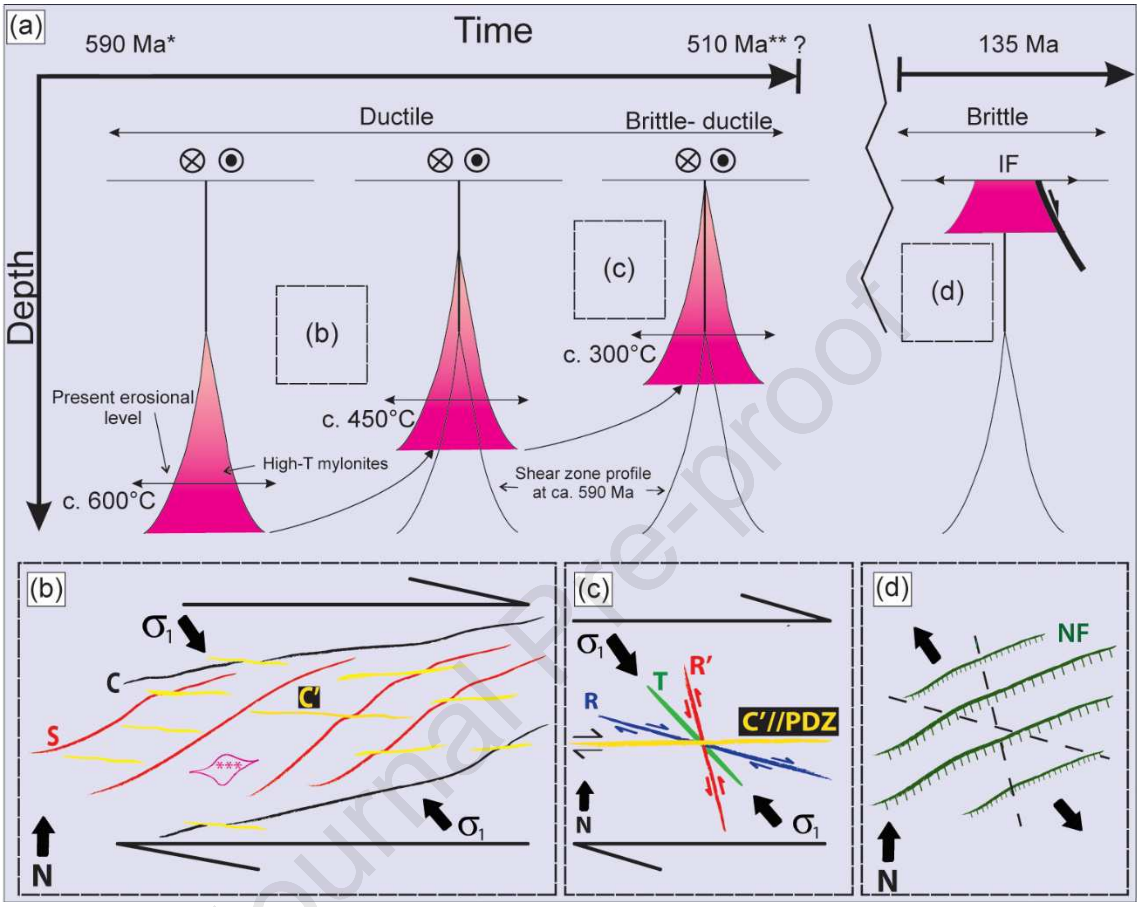

Figure 17. Schematic evolution model of the Cruzeiro do Nordeste shear zone. (a) Cooling-related exhumation brings high-T mylonites to progressive shallower levels, leading to their overprint by low temperature mylonites and then by brittle-ductile faults. During the Cretaceous, reactivation of the CNSZ generates the Ibimirim Fault (IF). Age estimates are based on LA-ICP-MS U-Pb zircon age of a syntectonic granite of the Vila Moderna Intrusive Suite (Santos, 2012)* and $^{40}Ar/^{39}Ar$ muscovite cooling age of a shear zone nearby to the CNSZ (Hollanda et al., 2010)**. (b and c) Inferred orientation of the regional main compressive stress (σ1). (b) Ductile fabrics showing S-C-C' foliations and σ- feldspar porphyroclast***. (c) Rield shear system showing the progressive deformation during the brittle-ductile transition (R, synthetic fault; R',

anthythetic fault; T, vein; PDZ, principal displacement zone. (d) S-C foliation and brittle-ductile faults are overprinted by a system of faults that represent the brittle reactivation of the CNSZ. The black arrows in (d) represent the extension direction. NF, normal fault.The CNSZ is represented by a subvertical mylonitic foliation striking ENE-WSW with a sub-horizontal stretching lineation (Fig. 3). Simple shear deformation under progressively shallower crustal levels produced an abundance of meso- and microscale structures, with microstructures recording deformation under continuous declining temperature from c. 650°C to c. 300°C (Fig. 17a). In the mylonitic orthogneiss and granite mylonites, crystal-plastic deformation and dynamic recrystallization of feldspars, myrmekite growth along the boundaries of K-feldspar porphyroclasts, and embayed quartz-quartz boundaries (Figs. 11 and 12) indicate that ductile deformation started under high-T conditions (> 550°C; Olsen and Kohstedt, 1985; Simpson and Wintsch, 1989; Miller and Paterson, 1994; Stipp et al., 2002; Mainprice et al., 1986). In the granite mylonites, in some parts of the mylonitic orthogneiss and in mylonites derived from the Vila Moderna Intrusive Suite, quartz ribbons, which define C planes, show dynamic recrystallization dominantly by subgrain rotation (Figs. 11-13), indicating deformation at moderate temperatures (c. 500-400 °C; Stipp et al., 2002). In finer-grained C- and C'-type shear bands, quartz recrystallized mostly by bulging and cataclastic deformation of feldspar is ubiquitous, indicating deformation down to c. 300 °C (Figs. 11e, 12d, 13c, d).

The ductile fabrics are crosscut by a system of brittle-ductile conjugate pair of WNW-ESE and N-S strike-slip faults, dextral and sinistral, respectively. At the mesoscale, curvature of the mylonitic foliation towards the faults indicates that shearing initiated under ductile conditions (Fig. 7). At the microscale, a component of plastic flow is indicated by rotation of quartz ribbons toward the fractures (Figs. 11g, h). The

E-W dextral brittle-ductile C’ shear bands (Figs. 6 and 8) are interpreted as the principal displacement zone (PDZ or Y) of the brittle-ductile transition (Fig. 8d and 17c). Furthermore, the T-type fracture (quartz veins) oriented NW-SE are localized on the bisectrix of the acute angle of the conjugate pair of the Riedel shear fractures. This strike-slip fault geometry supports a NE-SW extension and NW-SE shortening orientations. This structural context is consistent with the dextral sense of shear (MacClay, 1987; Davis et al., 2000). The absence of reactivation of the main mylonitic foliation at this stage can be related to its orientation with respect to σ1 in the brittle regime. The high angle between the foliation and σ1 is unfavorable for slip and failure thus took place across the foliation, forming R and R’ shears.

The above observations suggest that shearing has continued into the early Paleozoic during the late stages of the Brasiliano-Pan-African Orogeny. ^{40}Ar□^{39}Ar ages demonstrate a systematic cooling of the Borborema Province and that the final stage of ductile deformation occurred at ca. 500 Ma (Hollanda et al., 2010; Neves et al., 2012; Araujo et al., 2014). In synthesis, the results indicate that, with time, the present erosional surface was brought to progressively shallower depths in an active shear zone, with strike-slip regime evolving through the brittle-ductile transition (Fig. 17).. A similar evolution has been proposed for a shear zone from Nigeria (Adeoti et al., 2017) and shear zone activity at upper crustal levels have been described in other shear zones from Borborema Province (Araújo et al., 2001; Hollanda et al., 2010; Castro et al., 2012). These observations indicate that the last stages of orogenic evolution in the Brasiliano-Pan-African belts were still dominated by strike-slip shearing, in contrast to many Phanerozoic orogens that are characterized by gravitational collapse (e.g., Dewey, 1988; Vanderhaeghe, 2012).

5.2 Basement inheritance structural control

Pre-existing intraplate shear zones can induce mechanical and rheological control that influence the geometry of fault-bounded basins (Osaigiede, et al., 2020). The ductile, brittle-ductile and brittle deformations of shear zones play an important role in the tectonic evolution of intraplate rift basins, such as the North Sea rift (e.g. Fossen, 2010; Osaigiede, et al., 2020), the West Africa (Modisi et al., 2000), the East Greenland rift system (Rotevatn et al., 2018), the Taranaki Basin, New Zealand (Collanega et al., 2019), and Rio do Peixe, Araripe, Sergipe-Alagoas and Pernambuco basins in northeastern Brazil (e.g. Araujo et al., 2018; Vasconcelos et al., 2019; Celestino et al., 2020).

Milani and Davison (1988) argued that the northern fault boundary of the Reconcavo-Tucano-Jabotá, Ibirmirim Fault, is controlled by the Pernambuco shear zone (PSZ). However, the rift geometry of the north border of Jatobá Basin shows a clearer structural control of the CNSZ, instead of PSZ. The CNSZ is represented as sharp magnetic anomalies and topographic lineaments that are consistent with the field data of the mylonitic foliation trend ENE-SSW. The Ibimirim Fault was previously interpreted on the basis of geophysical data (gravity and seismic) (Milani and Davison, 1988) and is parallel to the CNSZ. A recent magnetotelluric profile perpendicular to the Ibimirim Fault imaged it as a shallow southward dipping fault and the Jatobá Basin as a thin conductive layer extending to a maximum depth of 4 km (Santos et al., 2014). In this work, we suggest that the Ibimirim Fault cuts a complex path through the main protoliths (dioritic to granitic othogneisses, pegmatite muscovite granite and peralkaline granite) of the mylonites of the CNSZ. This fault was developed parallel to the mylonitic foliation and its damage zone overprints the SC foliation as a system of normal faults filled by calcite. Thus, the orientation of the normal faults and the development of slickenfibres along their slip surfaces implies a reactivation over the CNSZ.

The fault core of the conjugate pair of strike-slip faults comprises breccia and cataclasites filled by calcite (slickenfibres). These faults also acted as pre-existent basement weakness for the Jatobá rift phase (Fig. 17d). In this case, it is interpreted as a late (Valanginian) calcite mineralization due to fluid flow along the preexistent weakness made by the strike-slip fault planes. Nevertheless, during the interactions between hydrothermal fluids and surrounding rocks, changes of temperature and pressure can result in the precipitation of calcite that fill up the preexisting structures, such as SC foliation and strike-slip fault planes (Hu, et al., 2018).

Additionally, we observe that the basement brittle-ductile structural geometry may be responsible for the sigmoidal shape of the Reconcavo-Tucano-Jatobá rift system. Likewise, their strikes are parallel to the main direction (N-S) of the regional Recôncavo-Tucano graben and to the NW-SE transfer faults (e.g., Vaza-Barris and Jeremoabo Faults) (Destro et al., 2003; Milani and Davison, 1988).

In agreement with previous works (Milani and Davison, 1988; Heine et al., 2013; Peralta Gomes et al., 2018), our data support the NW-SE extension direction during the rift phase of the Jatobá Basin, which also suggests reactivation of the brittle-ductile strike-slip faults present in the basement rocks (Fig. 17d).

LA-ICP-MS dating of calcite slickenfibres from brittle fault plane yielded a Lower Cretaceous age (135 ± 4.7 Ma) for the brittle reactivation of the CNSZ. This age is overlapped by This age is overlapped by Early Cretaceous deposits that represent the lacustrine, fan delta and fluvio-eolic depositional systems that comprise the rift phase of the Jatobá Basin (Horn and Melo, 2016; Tomé et al., 2014; Carvalho et al., 2018). This sequence is interpreted as have been deposited in a failed intracontinental rift formed during the Gondwana break-up due to the opening of South Atlantic Ocean (Szatmari et al., 1987; Magnavita and Cupertino, 1988; Milani and Davison, 1988; Magnavita, 1992; Magnavita et al., 1994; Szatmari and Milani, 1999; Gordon et al., 2017; Heine et al., 2013). Thus, the age reported here agrees with the known timing of the initial opening of the South Atlantic Ocean and indicates that the regional brittle deformation is linked to this event.

6. Conclusion

Based on the interpretation of field and microstructural work and on geochronological (U-Pb calcite) data from the Cruzeiro do Nordeste shear zone in the Borborema Province (NE Brazil), we arrive at the following conclusions:

- Meso- and microscopic ductile kinematic indicators, such us asymmetric boudins, σ- and δ-type feldspar porphyroclasts, synthetic faults in fractured porphyroclasts, quartz-feldspar sigmoids, S-C-C' foliations, and asymmetric myrmekite growth around K-feldspar porphyroclasts clearly indicate dextral shearing of the CNSZ in deep crustal levels.
- Crystal plastic deformation mechanisms record deformation at declining temperature conditions (e.g., grain boundary migration → subgrain rotation → bulging recrystallization in quartz), indicating continuing functioning of the CNSZ during exhumation.
- A Riedel shear system marked by the ductile-brittle conjugate pair of strike-slip faults (R, dextral, WNW-ESE and R', sinistral, N-S), E-W dextral PDZ, and NW-SE T-fractures indicate that shearing has continued during the last stages of the Brasiliano-Pan-African Orogeny. No evidence was found for development of

normal faults at this stage, indicating that extensional collapse did not play any role on the exhumation of this portion of Borborema Province.

- Mylonitic foliation planes and brittle-ductile faults were reactivated during the Cretaceous. U-Pb dating of fault-hosted calcite constrains this brittle reactivation to the age of 135 Ma (Valanginian), which is associated with opening of the South Atlantic Ocean and the rift phase of the Jatobá Basin.

Acknowledgments

We are grateful to the undergraduate students from the Department of Geology UFPE for the fruitful discussion during many fieldworks to the study area, in particular Paulo Castellan Medeiros and Dionísio Casimiro. Figure 3 is partly based on the geological maps produced as part of their graduation reports. We thank the Geochronology and Tracers Facility, British Geological Survey, Environmental Science Centre. We also thank CPRM – Serviço Geológico do Brasil – for providing access to geophysical data for academic purposes. We thank the Editor Stephen Laubach and the three anonymous reviewers for their helpful comments, which greatly improved the early version of this manuscript. This work represents the contribution N. 02 of the Laboratório de Modelagem de Bacias (ModLad-UFPE).

References

Adeoti, B., Okonkwo, C.T., 2017. Structural evolution of Iwaraja shear zone, southwestern Nigeria. Journal of African Earth Sciences 131, 117–127.

Angen, J. J., Van Staal, C. R., Lin, S., Nelson, J. L., Mahoney, J. B., Davis, D. W., McClelland, W. C., 2014. Kinematics and timing of shear zone deformation in the western Coast Belt: Evidence for mid-Cretaceous orogen-parallel extension. Journal of Structural Geology, 68, 273-299.

Araújo, M.N.C., Alves da Silva, F.C., Sá, J.d., 2001. Pegmatite emplacement in the Seridó belt, northeastern Brazil: late stage kinematics of the Brasiliano Orogen. Gondwana Research 4, 75-85.

Araujo, R.E.B., Bezerra, F.H.R., Nogueira, F.C.C., Balsamo, F., Carvalho, B.R.B.M., Souza, J.A.B., Sanglard, J.C.D., de Castro, D.L., Melo, A.C.C., 2018. Basement control on fault formation and deformation band damage zone evolution in the Rio do Peixe Basin, Brazil. Tectonophysics 745, 117–131.

Archanjo, C.J., Trindade, R.I.F., Bouchez, J.L., Ernesto, M., 2002. Granite fabrics and regional-scale strain partitioning in the Seridó Belt (Borborema Province, NE Brazil). Tectonics 21, 3-14.

Archanjo, C.J., Hollanda, M.H.B.M., Rodrigues, S.W.O., Brito Neves, B.B., Armstrong, R., 2008. Fabrics of pre- and syntectonic granite plutons and chronology of shear zones in the Eastern Borborema Province, NE Brazil. Journal of Structural Geology 30, 310-326.

Archanjo, C.J., Viegas, L.G.F., Hollanda, M.H.B.M., Souza, L.C., Liu, D., 2013. Timing of the HT/LP transpression in the Neoproterozoic Seridó Belt (Borborema Province, Brazil): Constraints from U\Pb (SHRIMP) geochronology and implications for the connections between NE Brazil and West Africa. Gondwana Research 23, 701-714.

Bezerra, F.H.R., Rossetti, D.F., Oliveira, R.G., Medeiros, W.E., Brito Neves, B.B., Balsamo, F., Nogueira, F.C.C., Dantas, E.L., Andrades Filho, C., Góes, A.M., 2014. Neotectonic reactivation of shear zones and implications for faulting style and geometry in the continental margin of NE Brazil. Tectonophysics 614, 78–90. https://doi.org/10. 1016/j.tecto.2013.12.021.

Blenkinsop, T.G., Treloar, P.J., 1995. Geometry, classification and kinematics of *S-C* and *S-C′* fabrics in the Mushandike area, Zimbabwe. Journal of Structural Geology 17, 397-408.

Brito Neves, B.B., Santos, E.J., Van Schmuss, W.R., 2000. Tectonic history of the Borborema Province. In: U.G. Cordani, E.J. Milani, A. Thomaz Filho and D.A. Campos (Editors), Tectonic evolution of South America. 31° International Geological Congress, Rio de Janeiro, pp. 151-182.

Carreras, J., Czeck, D.M., Druguet, E., Hudleston, P.J., 2010. Structure and development of an anastomosing network of ductile shear zones. Journal of Structural Geology 32, 656–666.

Carvalho, R.R. de, Neumann, V.H., Fambrini, G.L., Assine, M.L., Vieira, M.M., Rocha, D.E.G.A. da, Ramos, G.M.S., 2018. The basal siliciclastic Silurian-Devonian Tacaratu formation of the Jatobá basin: Analysis of facies, provenance and palaeocurrents. Journal of South American Earth Sciences 88, 94–106.

Castro, D.L., Bezeraa, F.H.R., Branco, R.M.G.C., 2008. Geophysical evidence of crustal-heterogeneity control of fault growth in the Neocomian Iguatu basin, NE Brazil. Journal of South American Earth Sciences 26, 271-285.

Castro, N.A., Ganade de Araujo, C.E., Basei, M.A.S., Osako, L.S., Nutman, A., Liu, D., 2012. Ordovician A-type granitoid magmatism on the Ceará Central Domain, Borborema Province, NE-Brazil. Journal of South American Earth Sciences 36, 18–31.

Celestino, M.A.l., Miranda, T.S., Mariano, G., Lima, M.A., Carvalho, B.R.B.M, Falcão, T.C., Topan, J.G., Barbosa, J.A., Gomes, I.F. 2020. Fault Damage Zones Width: Implications For The Tectonic Evolution Of The Araripe Basin, Brazil. Journal of Structural Geology, 138, 104-116.

Clerc, C. Ringenbach, J.C.., Jolivet, L., Ballard, J.F., 2017. Rifted margins: ductile deformation, boudinage, continentward-dipping normal faults and the role of the weak lower crust. Gondwana Research 53, 20-40.

Collanega, L., Siuda, K., Jackson, C.A.L., Bell, R. E., Coleman, A.J., Lenhart, A., Magee, C., Breda, A., 2019. Normal fault growth influenced by basement fabrics: The importance of preferential nucleation from pre□existing structures. Basin Research, 31, 659-687.

Corsini, M., Vauchez, A., Archanjo, C.J., Jardim de Sá, E.F., 1991. Strain transfer at acontinental scale from a transcurrent shear zone to a transpressional fold belt:the Patos-Seridó belt system, north-eastern Brazil. Geology 19, 586–589.

Corsini, M., Vauchez, A., Caby, R., 1996. Ductile duplexing at a bend of a continental-scale strike-slip shear zone: example from NE Brazil. Journal of Structural Geology 18, 385-394.

Davis, G. H., Bump, A. P., García, P. E., Ahlgren, S. G., 2000. Conjugate riedel deformation band shear zones. Journal of Structural Geology, 22, 169-190.

Destro, N., Alkmim, F. F., Magnavita, L. P., Szatmari, P., 2003. The Jeremoabo transpressional transfer fault, recôncavo–Tucano rift, NE Brazil. Journal of Structural Geology, 25(8), 1263-1279.

Dewey, J.F., 1988. Extensional collapse of orogens. Tectonics 7, 1123-1139.

Ferreira, J.M., Bezerra, F.H.R., Sousa, M.O.L., do Nascimento, A.F., Sá, J.M., França, G.S., 2008. The role of Precambrian mylonitic belts and present-day stress field in the coseismic reactivation of the Pernambuco lineament. Braz. Tectonophysics 456, 111–126.

Fossen, H., 2010. Extensional tectonics in the North Atlantic Caledonides: a regional view. Geological Society, London, Special Publications, 335, 767-793.

França, R.H.M., Neves, S.P., Bezerra, J.P.S., Bruguier, O., 2019. Geochemistry and geochronology of orthogneisses across a major transcurrent shear zone (East Pernambuco shear zone, Borborema Province, Northeast Brazil): Tectonic implications. Journal of South American Earth Sciences 91, 285-301.

Goldstein, A.G., 1988. Factors affecting the kinematic interpretation of asymmetric boudinage in shar zones. Journal of Structural Geology 10, 707-715.

Gordon, A., Destro, N., Heilbron, M., 2017. The Recôncavo-Tucano-Jatobá rift and associated Atlantic continental margin basins. In: Heilbron, M., Cordani, U.G., Alkmim, F.F. (Eds.), São Francisco Craton, Eastern Brazil, pp. 171–185.

Goscombe, B.D., Passchier, C.W., 2003. Asymmetric boudins as shear sense indicators - an assessment from field data. Journal of Structural Geology 25, 575-589.

Goscombe, B.D., Hand, M., Gray, D., 2003. Structure of the Kaoko Belt, Namibia: Progressive evolution of a classic transpressional orogen. Journal of Structural Geology 25, 1049-1081.

Guimarães, I.P., Da Silva Filho, A.F., Almeida, C.N., Van Schmus, W.R., Araújo, J.M.M., Melo, S.C., Melo, E.B., 2004. Brasiliano (Pan-African) granite magmatism in the Pajeú-Paraíba belt, Northeast Brazil: an isotopic and geochronological approach. Precambrian Research 135, 23-53.

Hanmer, S., 1986. Asymmetrical pull-aparts and foliation fish as kinematic indicators. Journal of Structural Geology 8, 111-122.

Hanmer, S., Passchier, C.W., 1991. Shear sense indicators: A review. Geological Survey of Canada 90, 1-71.

Heine, C., Zoethout, J., Müller, R.D., 2013. Kinematics of the South Atlantic rift. Solid Earth 4, 215–253.

Hollanda, M.H.B.M., Archanjo, C.J., Souza, L.C., Armstrong, R., Vasconcelos, P.M., 2010. Cambrian mafic to felsic magmatism and its connections with transcurrent shear zones of the Borborema Province (NE Brazil): Implications for the late assembly of the West Gondwana. Precambrian Research 178, 1-14.

Horn, B.L.D., Melo Ferrer de Morais, D., 2016. First occurrence of the Salvador Formation in the Jatobá Basin (Pernambuco, Northeast Brazil): Facies characterization and depositional systems. Journal of South American Earth Sciences 72, 25–37.

Hu, W., Wang, X., Zhu, D., You, Donghua, Wu, H., 2018. An overview of types and characterization of hot fluids associatetd with reservoir formation in petroliferous basin. Energy Exploration & Exploitation, 36, 1359–1375

Jadamec, M.A., Turcotte, D.L., Howell, P., 2007. Analytic models for orogenic collapse. Tectonophysics 435, 1-12.

Konopásek, J., Kroner, S., Kitt, S.L., Passchier, C.W., Kroner, A., 2005. Oblique collision and evolution of large-scale transcurrent shear zones in the Kaoko belt, NW Namibia. Precambrian Research 136, 139-157.

Leech, M.L., 2001. Arrested orogenic development: eclogitization, delamination, and tectonic collapse. Earth and Planetary Science Letters 185, 149-159.

Lister, G.S., Snoke, A.W., 1984. S-C mylonites. Journal of Structural Geology 6, 617-638.

Magnavita, L.P., 1992. Geometry and kinematics of the Recôncavo-Tucano-Jatobá Rift, NE Brazil. PhD Thesis. University of Oxford 493 pp.

Magnavita, L. P., Cupertino, J. A., 1988. A new approach to the geological configuration of the Lower Cretaceous Tucano and Jatobá basins, Northeastern Brazil. Revista Brasileira de Geociências, 18, 222-230.

Magnavita, L. P., Davison, I., Kusznir, N. J., 1994. Rifting, erosion, and uplift history of the Recôncavo□Tucano□Jatobá Rift, northeast Brazil. Tectonics 13, 367-388.

Mainprice, D., Bouchez, J.-L., Blumenfeld, P., Tubiá, J.M., 1986. Dominant *c* slip in naturally deformed quartz: Implications for dramatic plastic softening at high temperature. Geology 14, 819-822.

Mcclay, K. R., 1987. The mapping of geological structures. Geological Society of London 650 handbook.161.

Milani, E.J., Davison, I., 1988. Basement control and transfer tectonics in the Recôncavo-Tucano-Jatobá rift, Northeast Brazil. Tectonophysics 154, 41-50,53-70.

Miller, R.B., Paterson, S.R., 1994. The transition from magmatic to high-temperature solid-state deformation: implications from the Mount Stuart batholith, Washington. Journal of Structural Geology 16, 853-865.

Modisi, M. P., Atekwana, E. A., Kampunzu, A. B., Ngwisanyi, T. H., 2000. Rift kinematics during the incipient stages of continental extension: Evidence from the nascent Okavango rift basin, northwest Botswana. Geology, 28, 939-942.

Mukherjee, S., 2011. Mineral fish: Their morphological classification, usefulness as shear sense indicators and genesis. International Journal of Earth Sciences 100, 1013-1314.

Neves, S.P., 1991. A zona de cisalhamento Tauá, Ceará: sentido e estimativa do deslocamento, evolução estrutural e granitogênese associada. Revista Brasileira de Geociências 21, 161-173.

Neves, S.P, 2015. Constrains from zircon geochronology on the tectonic evolution of the Borborema Province: Widespread intracontinental Neoproterozoic reworking of a Paleoproterozoic accretionary orogen. Journal of South American Earth Sciences 58, 150-164.

Neves, S.P., Monié, P., Bruguier, O., Rangel da Silva, J.M., 2012. Geochronological, thermochronological and thermobarometric constraints on deformation, magmatism and thermal regimes in eastern Borborema Province (NE Brazil). Journal of South American Earth Sciences, v. 38, p. 129-146.

Neves, S.P., Mariano, G., 1999. Assessing the tectonic significance of a large-scale transcurrent shear zone system: the Pernambuco lineament, northeastern Brazil. Journal of Structural Geology 21, 1369-1383.

Neves, S.P., Vauchez, A., Feraud, G., 2000. Tectono-thermal evolution, magma emplacement, and shear zone development in the Caruaru area (Borborema Province, NE Brazil). Precambrian Research 99, 1-32.

Neves, S.P., Melo, S.C., Moura, C.A.V., Mariano, G., Silva, J.M.R., 2004. Zircon Pb-Pb geochronology of the Caruaru area, northeastern Brazil: temporal constraints on the Proterozoic evolution of Borborema Province. International Geology Review 46, 52-63.

Neves, S.P., Bruguier, O., Bosch, D., Silva, J.M.R., Mariano, G., 2008. U–Pb ages of plutonic and metaplutonic rocks in southern Borborema Province (NE Brazil): Timing of Brasiliano deformation and magmatism. Journal of South American Earth Sciences 25, 285-297.

Neves, S.P., Bruguier, O., Silva, J.M.R., Mariano, G., 2015. From extension to shortening: Dating the onset of the Brasiliano Orogeny in eastern Borborema Province (NE Brazil). Journal of South American Earth Sciences 58, 238-256.

Neves, S.P., Santos, T.A.S., Medeiros, P.C., Amorim, L.Q., Casimiro, D.C.G., 2018. Interference fold patterns in regional unidirectional stress fields: A result of local kinematic interactions. Journal of Structural Geology 115, 304-310.

Neves, S.P., Teixeira, C.M.L., Bruguier, O., 2020. Long-lived localized magmatism in the central-eastern part of Pernambuco-Alagoas Domain, Borborema Province (NE Brazil): Implications for tectonic setting, heat sources, and lithospheric reworking. Precambrian Research 337, 105559.

Roberts, N.M.W., Rasbury, E.T., Parrish, R.R., Smith, C.J., Horstwood, M.S.A., Condon, D.J., 2017. A calcite reference material for LA□ICP□MS U□Pb geochronology. Geochemistry, Geophysics, Geosystems 18, 2807-2814.

Ngako, V., Affaton, P., Nnange, J.M., Njanko, T., 2003. Pan-African tectonic evolution in central and southern Cameroon: transpression and transtension during sinistral shear movements. Journal of African Earth Sciences 36, 207-214.

Nogueira, F.C., Bezerra, F.H.R., Fuck, R.A., 2015. Quaternary fault kinematics and chronology in intraplate northeastern Brazil. Journal of Geodynamics 49, 79-91.

Olsen, T.S., Kohlstedt, D.L., 1985. Natural deformation and recrystallization of some intermediate plagioclase feldspars. Tectonophysics 111, 107-131.

Osagiede, E. E., Rotevatn, A., Gawthorpe, R., Kristensen, T. B., Jackson, C. A., Marsh, N., 2020. Pre-existing intra-basement shear zones influence growth and geometry of non-colinear normal faults, western Utsira High–Heimdal Terrace, North Sea. Journal of Structural Geology 130, 103908.

Paquette, J.L., Caby, R., Djouadi, M.T., Bouchez, J.L., 1998. U-Pb dating of the end of the Pan-African orogeny in the Tuareg shield: the post-collisional syn-shear Tioueine pluton (Western Hoggar, Algeria). Lithos 45, 245-253.

Passchier, C.W., Simpson, C., 1986. Porphyroclast systems as kinematic indicators. Journal of Structural Geology 8, 831-843.

Peralta Gomes, C., Fossen, H., de Almeida, R.P., Salmoni, B., 2018. Subseismic deformation in the Vaza-Barris Transfer Zone in the Cretaceous Recôncavo-

Tucano-Jatobá rift system, NE Brazil. Journal of Structural Geology 117, 81–95. 7

Ramsay, J.G., Huber, M., 1987. Folds and Fractures. In: The Techniques of Modern Structural Geology, vol. I. Academic Press, London.

Rey, P., Vanderhaeghe, O., Teyssier, C., 2001. Gravitational collapse of the continental crust: definition, regimes and modes. Tectonophysics 342, 435-449.

Rotevatn, A., Kristensen, T. B., Ksienzyk, A. K., Wemmer, K., Henstra, G. A., Midtkandal, I., Grundvåg, S.A.,,Andresen, A., 2018. Structural inheritance and rapid rift□length establishment in a multiphase rift: The East Greenland rift system and its Caledonian orogenic ancestry. Tectonics, 37, 1858-1875.

Santos, C.A., 2012. Cinturão de Cisalhamento Congo–Cruzeiro do Nordeste: Uma descontinuidade crustal no Domínio da Zona Transversal, Província Borborema. PhD thesis, Universidade Federal de Pernambuco, 126 p.

Santos, C.A., Accioly, A.C., 2010. Programa Geologia do Brasil. Carta Geológica – Escala 1:100 000: Folha SC.24-X-B-I, Sertânia. CPRM – Serviço Geológico do Brasil.

Santos E.J., Van Schmus W.R., Kozuch M., Brito Neves B.B. 2010. The Cariris Velhos Tectonic Event in Northeast Brazil. Journal of South American Earth Sciences 29, 61-76.

Santos, A.C.L., Padilha, A.L., Fuck, R.A., Pires, A.C.B., Vitorello, I., Pádua, M.B., 2014. Deep structure of a stretched lithosphere: Magnetotelluric imaging of the southeastern Borborema province, NE Brazil. Tectonophysics. 610, 39-50.

Santos, E.J., 1995. O complexo granítico de Lagoa das Pedras: acresção e colisão na região de Floresta (PE), Província Borborema. PhD thesis Thesis, Universidade de São Paulo.

Santos, E. J.; Vasconcelos, A. M., 1973. Características dos granitóides de tipo Moderna do Lineamento Pernambuco. Mineração Metalurgia 339, 28-33.

Santos, E.J., Ferreira, C.A., Silva Jr., J.M.F., 2002. Geologia e Recursos Minerais do Estado da Paraíba. Programa Levantamentos Geológicos Básicos do Brasil. CPRM – Serviço Geológico do Brasil.

Santos, L.C.M.L., Dantas, E.L., Cawood, P.A., Santos, E.J., Fuck, R.A., 2017. Neoarchean crustal growth and Paleoproterozoic reworking in the Borborema Province, NE Brazil: Insights from geochemical and isotopic data of TTG and metagranitic rocks of the Alto Moxotó Terrane. Journal of South American Earth Sciences 79, 342-363.

Silva, J.M.R., Mariano, G., 2000. Geometry and kinematics of the Afogados da Ingazeira shear zone, Northeast Brazil. International Geology Review 42, 86-95.

Simpson, C., Wintsch, 1989. Evidence for deformation-induced K-feldspar replacement by myrmekite. Journal of Metamorphic Geology 7, 261-275.

Souza, Z.S. et al., 2006. Eletron microprobe dating of monazite from high-T shear zones in the São José do Campestre Massif, NE Brazil. Gondwana Research 9, 441-455.

Stewart, M., Hosdsworth, R.E., Strachan, R.A., 2000. Deformation processes and weakening mechanisms within the frictional-viscous transition zone of major crustal-scale faults: insights from the Great Glen Fault Zone, Scotland. Journal of Structural Geology 22, 543-560.

Stipp, M., Stünitz, H., Heilbronner, R., Schmid, S.M., 2002. The eastern Tonale fault zone: a 'natural laboratoy' for crystal plastic deformation of quartz over a temperature range from 250 to 700 ºC. Journal of Structural Geology 24, 1861-1884.

Szatmari, P., Françolin, J. B. L., Zanotto, O., Wolff, S., 1987. Evolução tectônica da margem equatorial brasileira. Revista brasileira de Geociências, 17, 180-188.

Szatmari, P., Milani, E. J., 1999. Microplate rotation in northeast Brazil during South Atlantic rifting: Analogies with the Sinai microplate. Geology, 27, 1115-1118.

ten Grotenhuis, S.M., Trouw, R.A.J., Passchier, C.W., 2003. Evolution of mica fish in mylonitic rocks. Tectonophysics 372, 1-21.

Tomé, M.E.T.R., Lima, M.F., Neumann, V.H.M.L., 2014. Taxonomic studies of non-marine ostracods in the Lower Cretaceous (Aptian – lower Albian) of post-rift sequence from Jatobá and Araripe basins (Northeast Brazil): Stratigraphic implications. Cretaceous Research 48, 153–176.

Van Schmus, W.R., Oliveira, E.P., Da Silva Filho, A., Toteu, S.F., Penaye, J., Guimarães, I.P., 2008. Proterozoic links between the Borborema Province, NE Brazil, and the Central African Fold Belt. Geological Society, London, Special Publications 294, 69-99.

Van Schmus, W.R., Kozuch, M., Brito Neves, B.B., 2011. Precambrian history of the Zona Transversal of the Borborema Province, NE Brazil: Insights from Sm-Nd and U-Pb geochronology. Journal of South American Earth Sciences 31, 227-252.

Vanderhaeghe, O., 2012. The thermal–mechanical evolution of crustal orogenic belts at convergent plate boundaries: A reappraisal of the orogenic cycle. Journal of Geodynamics, 56, 124-145.

Vasconcelos, D.L., Bezerra, F.H.R., Medeiros, W.E., de Castro, D.L., Clausen, O.R., Vital, H., Oliveira, R.G., 2019. Basement fabric controls rift nucleation and postrift basin inversion in the continental margin of NE Brazil. Tectonophysics 751, 23–40.

Vauchez, A., Egydio-Silva, M., 1992. Termination of a continental-scale strike-slip fault in partially melted crust: The West Pernambuco shear zone, northeast Brazil. Geology 20, 1007-1010.

Vauchez, A., Neves, S.P., Caby, R., Corsini, M., Egydio-Silva, M., Arthaud, M.H., Amaro, V., 1995. The Borborema shear zone system, NE Brazil. Journal of South American Earth Sciences 8, 247-266.

Viegas, L.G.F., Archanjo, C., Vauchez, A., 2013. Fabrics of migmatites and the relationships between partial melting and deformation in high-grade transpressional shear zones: the Espinho Branco anatexite (Borborema Province, NE Brazil). Journal of Structural Geology 48, 45–56.

Viegas, L.G.F., Archanjo, C.J., Hollanda, M.H.B.M., Vauchez, A., 2014. Microfabrics and zircon U-Pb (SHRIMP) chronology of mylonites from the Patos shear zone (Borborema Province, NE Brazil). Precambrian Research 243, 1–17.

West, D.P., Jr., Hubbard, M.S., 1997. Progressive localization of deformation during exhumation of a major strike-slip shear zone: Norumbega fault zone, south-central Maine, USA. Tectonophysics 273, 185-201.

Woodcock, N.H., Mort, K.M., 2008. Classification of fault breccias and related fault rocks. Geological Magazine 145, 435–440.

Highlights:

- Continuous transition from ductile to brittle-ductile deformation in Brasiliano-age shear zone;
- Conjugate pair of strike-slip faults represents the cooler semi-brittle to brittle deformation;
- The Brasiliano-Pan-African Orogeny persisted well into the Paleozoic;
- U-Pb age of fault-hosted calcite constrains brittle reactivation to the age of 135 Ma.

Declaration of interests

☒ The authors declare that they have no known competing financial interests or personal relationships that could have appeared to influence the work reported in this paper.

☐The authors declare the following financial interests/personal relationships which may be considered as potential competing interests:

The authors whose names are listed in the manuscript file certify that they have NO financial interest (such as personal or professional relationships, affiliations, knowledge or beliefs) in the subject matter or materials discussed in this manuscript.